

ABSTRACT

ARMES, ROBERT J. Aerodynamic Fuselage Design and Engine Integration for the Vampire Light Sport Aircraft. (Under the direction of Dr. Charles E. Hall Jr.)

This paper covers the design of a new fuselage and the integration of the Rotax 912 ULS engine for the Vampire Light Sport Aircraft. The Vampire is a side-by-side two-seat pusher configuration currently owned by LSA America. The primary goals were to reduce the base drag of the existing prototype's composite fuselage and to make provisions for adequate cooling of the engine. To accomplish these goals within the project's scope and timeline, an analysis method using Fluent and the ANSYS 13 Workbench suite was developed. To evaluate drag, the fuselage and a 2-volume computational domain were modeled in SolidWorks. A mesh was generated in the Workbench mesh tool using manual element sizing controls, and the flow was simulated in Fluent using the Spalart-Allmaras turbulence model. The method was validated by comparing the drag results of a sphere to experimental data. Using the method in an iterative design process, a drop-in replacement fuselage for the Vampire was designed that reduces drag by 11.5% and as a result reduces the power required at a velocity of 120kts by 4.4hp. The new design was accomplished by modifying only the fuselage section aft of the firewall; this eases production of the new fuselage by only requiring the addition of plugs to the existing molds. After the external lines of the new fuselage were determined, the integration of the Rotax 912 ULS engine was performed. It was assumed that the stock frame and exhaust system as described in its installation manual would be used. In this application, the computational domain was modeled as a single volume and meshed in the Workbench mesh tool using a mix of automatic features and element size controls. The flow was simulated in Fluent using the Spalart-Allmaras turbulence model. Feedback from the flow visualization results allowed for ram air intake scoops and baffles to be designed such that cooling airflow reached critical engine components.

© Copyright 2013 by Robert J. Armes

All Rights Reserved

Aerodynamic Fuselage Design and Engine Integration for the
Vampire Light Sport Aircraft

by
Robert J. Armes

A thesis submitted to the Graduate Faculty of
North Carolina State University
in partial fulfillment of the
requirements for the degree of
Master of Science

Aerospace Engineering

Raleigh, North Carolina

2013

APPROVED BY:

Dr. Charles E. Hall Jr.
Committee Chair

Dr. Ashok Gopalarathnam

Dr. James Selgrade

DEDICATION

I dedicate this thesis to my loving parents and sister – Nigel, Vicki, and Phillipa Armes. Thank you for being there for me whenever I needed encouragement and a comforting home-cooked meal. I also dedicate this work to my high school mentor and aerospace teacher, Michael Kelley. Without your inspiration and guidance, I would not have found my passion for aviation and aircraft design.

BIOGRAPHY

Robert Armes was born in Kent, England to Nigel and Vicki Armes. At the age of two, he moved to Hyderabad, India where his younger sister, Phillipa, was born. After spending six years in India, the Armes family spent another six years in Singapore before moving to Raleigh, North Carolina in 2002. Robert gained an interest in aviation in his freshman year at Leesville Road High School. Leesville offered an aerospace class series where Robert learned how to build and fly remote-controlled aircraft. After graduating from Leesville in 2007, he completed his B.S. in Aerospace Engineering at NC State University and immediately began work on his M.S. degree. He has spent his time as a graduate student as a teaching assistant for the department's Aircraft Senior Design course and performing design work for the Vampire Light Sport Aircraft for which this thesis is written. Upon graduating with his Master's Degree, he plans on going into industry where he can apply his engineering knowledge and aircraft design experience.

ACKNOWLEDGMENTS

I would like to thank Dr. Charles Hall for giving me the opportunity to be a part of Flight Research and supporting me throughout my graduate career. His advice and guidance have been key to the success of this research.

I would like to thank my parents and my sister, whose encouragement and support has helped me get through rough times and motivated me to achieve anything I set my mind to.

I would like to thank the members of Flight Research – Stearns, Lars, and Alex. Without the distractions and spontaneous experiments, the hours spent in the lab would not have been nearly as enjoyable.

I would like to thank Doug Hempstead at LSA America for choosing NC State University to assist in the design work of the Vampire Light Sport Aircraft. Had he decided to go elsewhere, I would not have had the opportunity to participate in this design project.

TABLE OF CONTENTS

LIST OF TABLES	vii
LIST OF FIGURES	viii
1 Introduction.....	2
1.1 Brief History.....	2
1.2 Identified Areas for Improvement.....	4
1.3 Project Scope.....	6
2 Analysis Method	7
2.1 CFD for External Fuselage Design	8
2.1.1 CAD Modeling.....	8
2.1.2 Meshing.....	10
2.1.3 Fluent Set-Up.....	15
2.2 Fuselage CFD Method Validation.....	16
2.3 CFD for Internal Flow Modeling.....	19
2.3.1 CAD Modeling.....	19
2.3.2 Meshing.....	21
3 Fuselage Design	23
3.1 Establishing the Baseline	24
3.2 Dimension Constraints	27
3.3 New Design Configurations	30
3.3.1 Version 1	32
3.3.2 Version 2.....	33
3.3.3 Version 3 - Final	34
4 Engine Integration.....	37
4.1 Engine Positioning	37
4.2 Cooling Airflow	39
5 Additional Considerations	44
5.1 Full Assembly	44
5.1.1 Propeller Clearance.....	45
5.2 Estimated Weight Impacts	46
5.3 Mold Plug.....	49

6	Conclusion	51
6.1	Future Work	52
6.2	Concluding Remarks	53
	References.....	54
	Appendix.....	56
	Appendix A – Method User Guide	57
	Appendix B – Intermediate CFD Results	61
	Appendix C – Intermediate Internal Flow CFD Results.....	63
	Appendix D – Cooling Component Geometry	65
	Appendix E – New Vampire 3-View.....	69

LIST OF TABLES

Table 2-1: Element Size Control Values	12
Table 2-2: Sphere Reference Values.....	18
Table 3-1: Baseline Fuselage Reference Values.....	25
Table 3-2: New Fuselage Configuration Comparison	31
Table 5-1: Weight Impact Summary.....	48
Table 5-2: Performance Estimate Summary	48
Table 5-3: Mold Plug Statistics.....	50
Table D-1: Upper Intake Scoop Statistics.....	65
Table D-2: Lower Intake Scoop Statistics	66

LIST OF FIGURES

Figure 1-1: Original 2008 Vampire Prototype.....	3
Figure 1-2: Second Vampire Prototype	3
Figure 1-3: Jabiru 3300 installed in Vampire Prototype.....	5
Figure 1-4: Blunt Fuselage Aft Section	5
Figure 2-1: CAD Modeling Process for CFD Domain	9
Figure 2-2: Two-Part CFD Domain.....	10
Figure 2-3: Named Selections – Inlet (left) and Outlet (right)	11
Figure 2-4: Named Selection – Symmetry (left) and Aircraft (right).....	11
Figure 2-5: Named Selection – Interface (left) and Farfield (right)	11
Figure 2-6: Computational Domain Dimensions	13
Figure 2-7: Vampire Fuselage CFD Mesh.....	14
Figure 2-8: Vampire Fuselage CFD Mesh Close-Up	14
Figure 2-9: Turbulence Model Comparison	15
Figure 2-10: Sphere Drag Validation Mesh.....	17
Figure 2-11: Sphere Drag Validation Velocity Rendering	18
Figure 2-12: Sphere Drag Validation Pressure Rendering	19
Figure 2-13: Creating the Internal Flow Computational Domain.....	20
Figure 2-14: Internal Flow Model Assembly.....	21
Figure 2-15: Example Internal Flow Mesh.....	22
Figure 3-1: Baseline Fuselage Major Dimensions.....	24
Figure 3-2: Baseline Fuselage Velocity Contours (120kts).....	25
Figure 3-3: Baseline Fuselage Pressure Contours (120kts)	26
Figure 3-4: Internal Wing Structure.....	27
Figure 3-5: Wing Trailing Edge Detail.....	28
Figure 3-6: Width Constraints	30
Figure 3-7: New Fuselage Configuration Options.....	31
Figure 3-8: Rear and Side View for New Fuselage v1	32

Figure 3-9: Rear and Side View for New Fuselage v2	33
Figure 3-10: Rear and Side View for Final Configuration	34
Figure 3-11: New Fuselage CFD Velocity Contours.....	35
Figure 3-12: New Fuselage CFD Pressure Contours	35
Figure 4-1: Rotax 912 ULS Engine (right) and CAD Model (left)	38
Figure 4-2: Engine Position in Engine Compartment.....	38
Figure 4-3: Upper Intake Scoop.....	40
Figure 4-4: Upper Baffle Location	41
Figure 4-5: Lower Intake Scoop	42
Figure 4-6: Lower Baffles.....	42
Figure 4-7: Internal Flow Results for Final Baffle and Inlet Scoop Configuration.....	43
Figure 5-1: New Fuselage Integrated with the Wing and Tail Components	44
Figure 5-2: Propeller Clearance	45
Figure 5-3: Allegro Composite Sandwich	46
Figure 5-4: New and Prototype Fuselage Aft Section Comparison.....	49
Figure 5-5: CAD Model for Mold Plug	49
Figure B-1: New Fuselage v1 Velocity Results.....	61
Figure B-2: New Fuselage v1 Pressure Results	61
Figure B-3: New Fuselage v2 Velocity Results.....	62
Figure B-4: New Fuselage v2 Pressure Results	62
Figure C-1: Un-Baffled Internal Flow	63
Figure C-2: Internal Flow with Single Upper Baffle	63
Figure C-3: Internal Flow with Upper Baffle and Small Lower Inlet	64
Figure C-4: Mesh for Final Internal Flow Simulation	64

1 Introduction

1.1 Brief History

The Vampire is a small 2-seat pusher configuration aircraft that will be marketed in the Federal Aviation Administration's (FAA) newest aircraft category of Light Sport Aircraft (LSA). This category was established to encompass simple small aircraft that would require less training for pilots to fly; these appeals to both new and experienced pilots as it is less costly and does not require a Class III medical certificate. Aircraft in this category must conform to the following FAA airworthiness criterion [1]:

- Maximum takeoff weight (MTOW) not to exceed 1320 lbs.
- Maximum allowable calibrated airspeed of 120 kts.
- If powered, may only be a single reciprocating engine with a fixed-pitch or ground-adjustable propeller.
- Landing gear must be fixed.
- Maximum stall speed of 45 kts in the clean configuration.
- Maximum seating capacity of 2 including the pilot.

Not to be confused with the original single-seat Vampire experimental aircraft produced by Sadler Aircraft Corporation in the early 1980's, the current Vampire's design instead drew heavily from a previous Sadler Aircraft design, the Piranha. It is characterized by twin tail-booms, a large horizontal stabilizer, and spacious cabin with side-by-side seating for the pilot and passenger. The original 2008 Vampire prototype was also intended to have foldable wings for easy storage, as shown in Figure 1-1 on the next page.

Due to financial reasons and lack of investor funding, Sadler Aircraft Company sold the rights to the Vampire design in 2010 along with the prototype they had in their possession at the time [2]. It was purchased by LSA America, a North Carolina based company known for the Allegro Light Sport Aircraft.



Figure 1-1: Original 2008 Vampire Prototype



Figure 1-2: Second Vampire Prototype

1.2 Identified Areas for Improvement

The second Vampire Prototype, which is currently in LSA America's possession, has a few problems and design features that the company wishes to change to make the aircraft more marketable and easier to manufacture by means of sharing common components with the Allegro LSA and utilizing existing tooling in LSA America's production line. The company approached the NC State Mechanical and Aerospace department for assistance in the re-design of the Vampire aircraft. After an inspection of the prototype, the following areas were identified for improvement:

The installed power-plant is a Jabiru 3300 6-cylinder reciprocating engine. Due to the positioning of the engine and length of the aft fuselage, a counter-balanced extension shaft is required to connect the propeller and spinner to the output shaft of the engine. For cooling, there are two side-mounted scoops that draw in ram air that is re-directed forwards over the cylinders and then down and out of the fuselage (Figure 1-3). The ribbed ducting and reversal of the cooling flow direction relative to the free stream introduces inefficiencies, and LSA America reports that the prototype has cooling issues when the engine is run at high throttle settings and at idle when stationary. Furthermore, the 6-cylinder engine may also be oversized for the LSA application which also means that the heavier engine subtracts useful payload capability from the LSA MTOW weight limit. To address these issues, LSA America requested that the engine be substituted with the Rotax 912 ULS – the same engine used in the Allegro.



Figure 1-3: Jabiru 3300 installed in Vampire Prototype

Next, the aft section of the fuselage ends in a steep blunt face so that the fuselage lines can close and converge from the low wing to the high-mounted propeller (Figure 4). This geometric feature leads to highly separated airflow and adverse pressure gradients that cause more drag which in turn reduces fuel efficiency and performance.

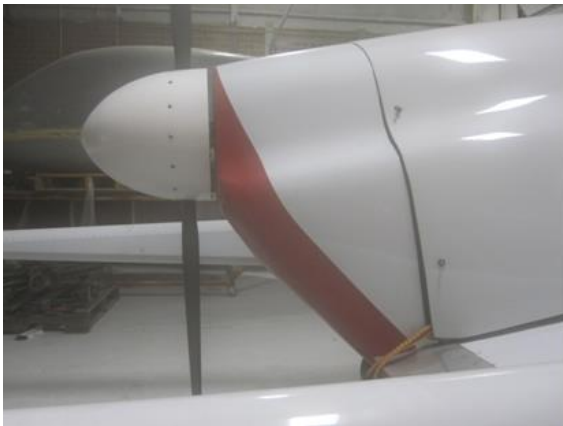


Figure 1-4: Blunt Fuselage Aft Section

The fuselage was manufactured using a chopped-fiberglass fiberglass layup, identical to a layup used in recreational boat construction. This type of composite layup is very heavy and overbuilt for an aircraft application. LSA America reported that due to the heavy fuselage, the 1320lbs MTOW limit was exceeded when the aircraft was fully loaded with two occupants on board.

The fixed trailing link landing gear is fabricated from steel tubing and plates that are welded together. The material and gauge of the components are capable of handling structural loads of a much larger aircraft, and are therefore adding unnecessary weight to the Vampire.

Lastly, LSA America expressed a desire to delete the folding wing feature. This would make the wings easier to manufacture if they were one-piece with a continuous spar. It would also eliminate any operator safety risks should pilots forget to secure the wings in the extended position before take-off. Such a feature change would require re-design of the wing structure.

1.3 Project Scope

It was the scope of this project to address the aerodynamic design of the fuselage and integration of the Rotax 912 ULS engine - including provisions for adequate cooling airflow. To re-shape the fuselage, Computational Fluid Dynamics (CFD) was used to more accurately capture the pressure effects of bluff geometry features and the low-wing configuration that normally would be made difficult and time consuming if done analytically. Computer-Aided Design (CAD) tools such as SolidWorks was used to perform the design and integration work as well as generate models that can be meshed for CFD simulations. To address engine cooling airflow, CFD was used to model airflow internal to the engine compartment such that baffles can be designed and positioned to direct the airflow over critical cooling components. It was the goal of this thesis to develop and utilize a CFD method that allows for relatively fast and accurate analysis in the aforementioned applications that can be implemented by engineers with little to no experience in CFD.

2 Analysis Method

LSA America provided the CAD files for the Vampire prototype. Since these files were generated by Sadler Aircraft in SolidWorks, it made sense to continue the design work in the same CAD suite. Several CFD packages were investigated for use with this project, including SolidWorks' FlowSim and Fluent. It was decided that Fluent in the ANSYS 13 suite would be used since a full version of the SolidWorks FlowSim was not available to the university. Furthermore, Fluent is integrated into ANSYS Workbench which packages modeling, meshing, and post processing in a single interface. Being able to access all of these features from a single user interface streamlines the process and allows for faster turn-around times in iterative design processes.

In CFD applications, the fluid volume around the part that is being analyzed must be modeled – not the part itself. It is common practice in CFD to model large volumes around the part in question because the effects of pressure and velocity can often reach into the far-field of the domain. The computational domain is divided into smaller parts, called elements, in the meshing step. Typically, the smaller the elements, the more accurate the solution will be. This becomes an important principle to follow when meshing models for CFD simulation, as the elements must be small enough near the boundary layer to resolve it to get accurate drag and lift results. In summary, this means that for a CFD simulation to more accurately represent real-world flow, the computational domain must be large and the element size must be small; this also means that meshes with a very large number of elements is required. However, it was found during the method development phase of this project that the ANSYS Fluent student license limits the user to simulations with meshes of no more than about 1.5 million elements. This limit became difficult to work around, but the meshing methods detailed later in this section present a way to generate meshes using the ANSYS Workbench meshing tool to arrive at practical results.

2.1 CFD for External Fuselage Design

It was found that the modeling step was made easier by the ANSYS Workbench Design Modeler tool where solid volumes could be subtracted from each other. These allowed the user to model both the part and the domain as separate solids. To obtain just the fluid volume, the user could then subtract the part volume from the domain once the part was properly positioned in the domain via an assembly. This process is detailed later in this section. The next step was to mesh the domain using the ANSYS Workbench meshing tool.

Unlike traditional more commonly used CFD meshing tools, the Workbench mesher did not have as many fine control features to create a mesh that is ideal for CFD analysis. By using only a single-piece domain, it was difficult to mesh a model such that the elements near the part were small to capture the boundary layer and elements in the far-field were larger where pressure and velocity gradients are less severe. It was also very difficult to set-up the mesher to have a fine mesh in the wake of the part where separated flow and turbulence were expected to occur. However, if the domain was divided into multiple volumes in the SolidWorks assembly, the mesher could be commanded to generate different element sizes for different volumes of the domain once it was imported.

Once a suitable mesh was generated, it was loaded into ANSYS Fluent and the simulation was set-up. The 1-equation Spalart-Allmaras (S-A) turbulence model was used for its faster computation times and reasonable results that were validated against experimental wind tunnel data.

2.1.1 CAD Modeling

In design applications, engineers usually model a part, such as a fuselage, as it would appear when fabricated. In CFD, however, the volume around the part must be modeled - like in a negative mold. Modeling for computational domains in CFD in CAD suites like SolidWorks is not as straight forward as one would think, and the extra time and effort it takes to use the mold tools or creating a separate model for CFD could easily discourage anyone wanting to

perform CFD analysis on their designs. However, if one looks beyond using only SolidWorks to model the computational domain, the ANSYS Workbench Design Modeler has a volume subtracting feature that makes this process simple. In addition to the part that the user wants to analyze in CFD, the user only needs to model a volume representing the computational domain. They can be imported to the Design Modeler as a SolidWorks assembly, and the volume of the part can be subtracted from the computational domain using the ‘Boolean Subtract’ command. Figure 2-1 depicts this process. Since fuselages are generally left-right symmetric, only half of the fluid domain was modeled for all cases in this project. This reduces the total computational domain volume and allows for a more refined mesh when working under an element limit.

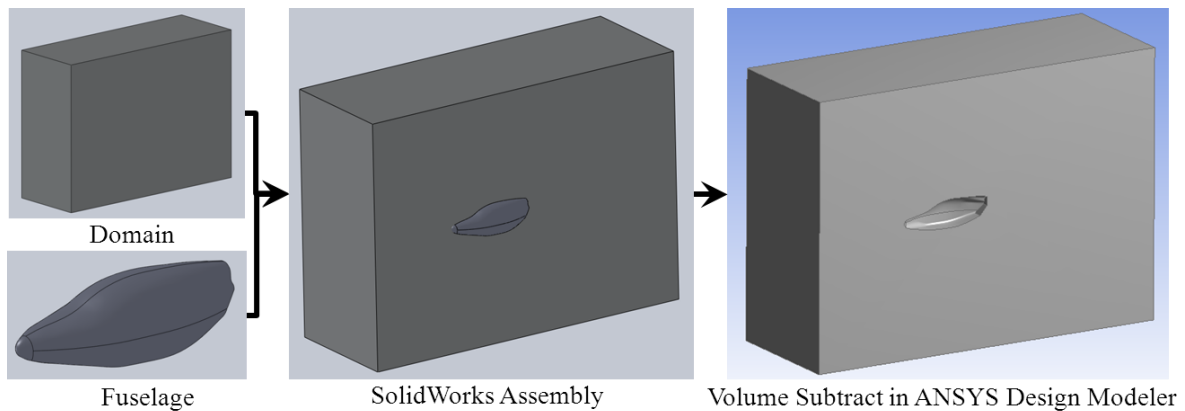


Figure 2-1: CAD Modeling Process for CFD Domain

Figure 2-1 above depicts the original Vampire fuselage in the computational domain. Using this model, it was found to be very difficult to generate a mesh that was fine at the boundary layer, coarse in the far-field, and fine in the wake behind the fuselage. Instead, a two-volume approach shown in Figure 2-2 on the following page was used. The domain (blue) remained of the same dimension, but instead of being a single piece, a core-section (yellow) around the fuselage (red) extending to the outlet of the domain was added. In the meshing step, this allows for additional surfaces and volumes where element size controls can be implemented to refine the mesh in areas of interest. It is important to note that when modeling the two

volumes in CAD, their surfaces must be coincident in the assembly so that there are no gaps in the computational domain.

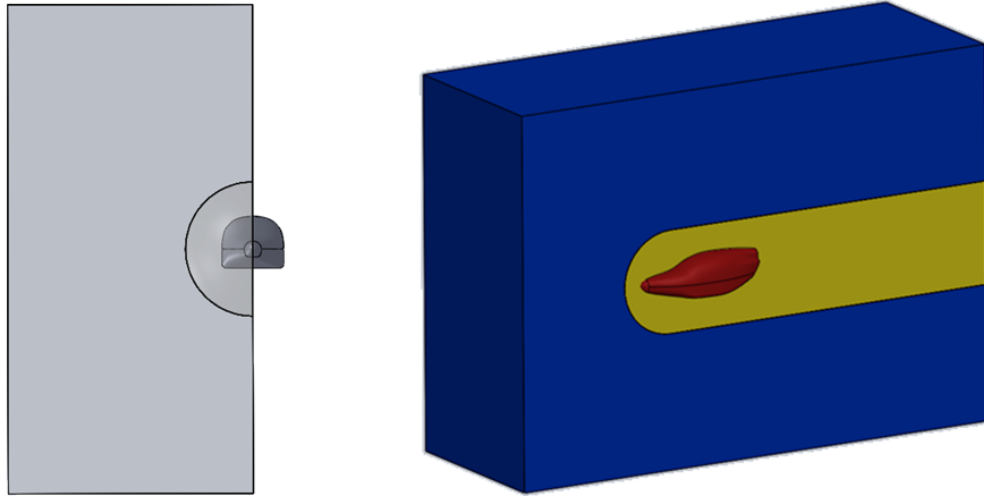


Figure 2-2: Two-Part CFD Domain

2.1.2 Meshing

Once the computational domain was modeled and the fuselage part has been subtracted from the domain volume in the design modeler, the next step was to mesh the domain. This was done using the ANSYS Workbench mesh tool. Meshing consisted of two steps: the first step was to define named surface selections. Performing this step allowed Fluent to automatically detect which faces are inlets, outlets, symmetry planes, and walls. It also allows the user to select groups of faces, such as the fuselage, on which you can monitor drag and lift forces. The second step was creating element size controls on key surfaces. This step allowed control of the fineness of the mesh in important areas and also allowed for tailoring of the mesh so that it remained in the 1.5 million element limit of the ANSYS student license restriction. The following figures show an example of how named selections were designated on a mesh for an iteration of the re-designed Vampire fuselage.

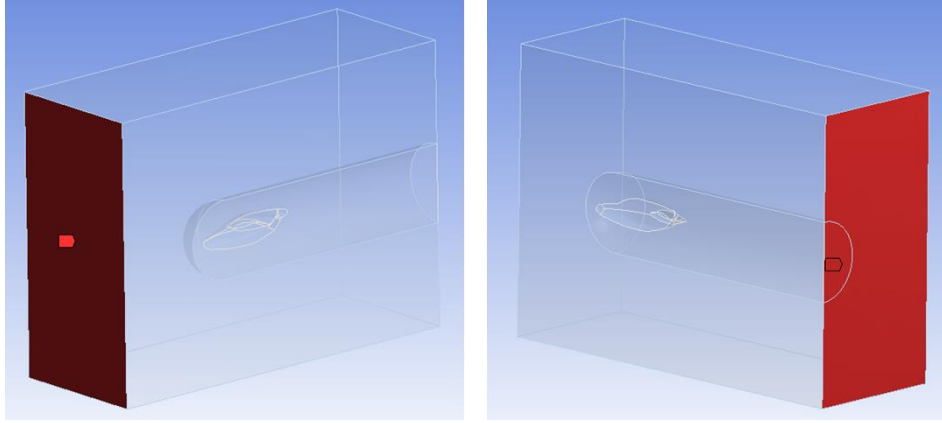


Figure 2-3: Named Selections – Inlet (left) and Outlet (right)

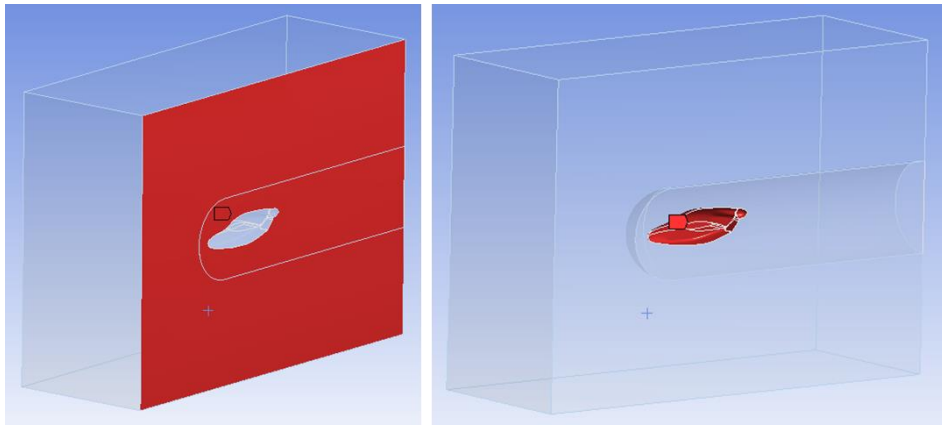


Figure 2-4: Named Selection – Symmetry (left) and Aircraft (right)

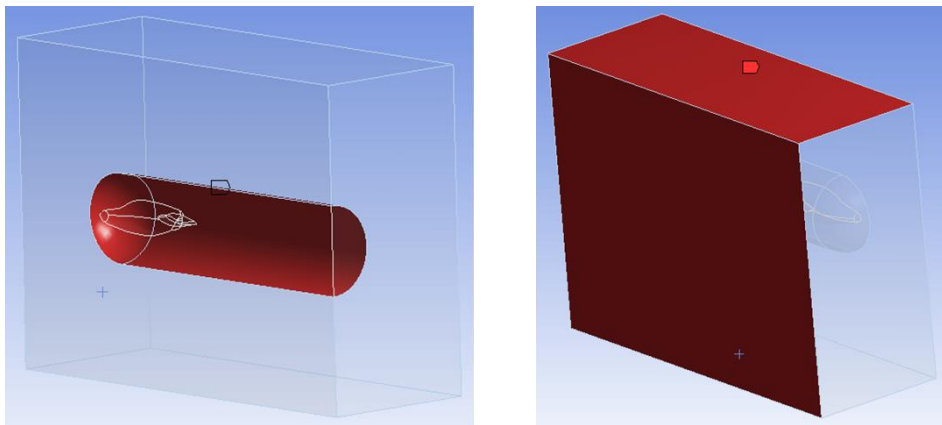


Figure 2-5: Named Selection – Interface (left) and Farfield (right)

It was important that separate named selections for the interface surfaces on both the domain and the wake core were made. For example, an interface named ‘interface-domain’ was made on the domain body, and a separate selection named ‘interface-wake’ was made on the wake-core body. This was required for the Fluent application to link the two bodies together in the mesh so they become one fluid volume. It also helped to name the surface selections using the naming convention given in the figure captions. The Fluent application automatically recognized the ‘inlet’, ‘outlet’, ‘symmetry’, and ‘interface’ keywords and automatically assigned the appropriate boundary conditions to them when the mesh was imported. This reduced the user workload and made the process faster.

Using the aforementioned named selections, element size controls were implemented so that the desired mesh geometry was obtained. General sizing guidelines were developed using a trial-and-error approach where computational domain volume was balanced with element size on the various surfaces so that the mesh was fine enough to produce meaningful results while remaining under the 1.5 million element limit for the student license. Figure 2-6 on the following page depicts the final dimensions for the computational domain and the corresponding element size controls are listed in the following table. Note that the reference chord is 62”, the chord of the Vampire wing. Note the listed element sizing is in meters since the ANSYS Workbench mesh tool defaults to metric dimensioning. The percent-chord values are given so they can be used in other applications.

Table 2-1: Element Size Control Values

Surface	Far-Field & Inlet	Outlet	Interface	Aircraft
Element Size (m)	0.35	0.15	0.07	0.015
% Chord	22	9.5	4.4	0.95

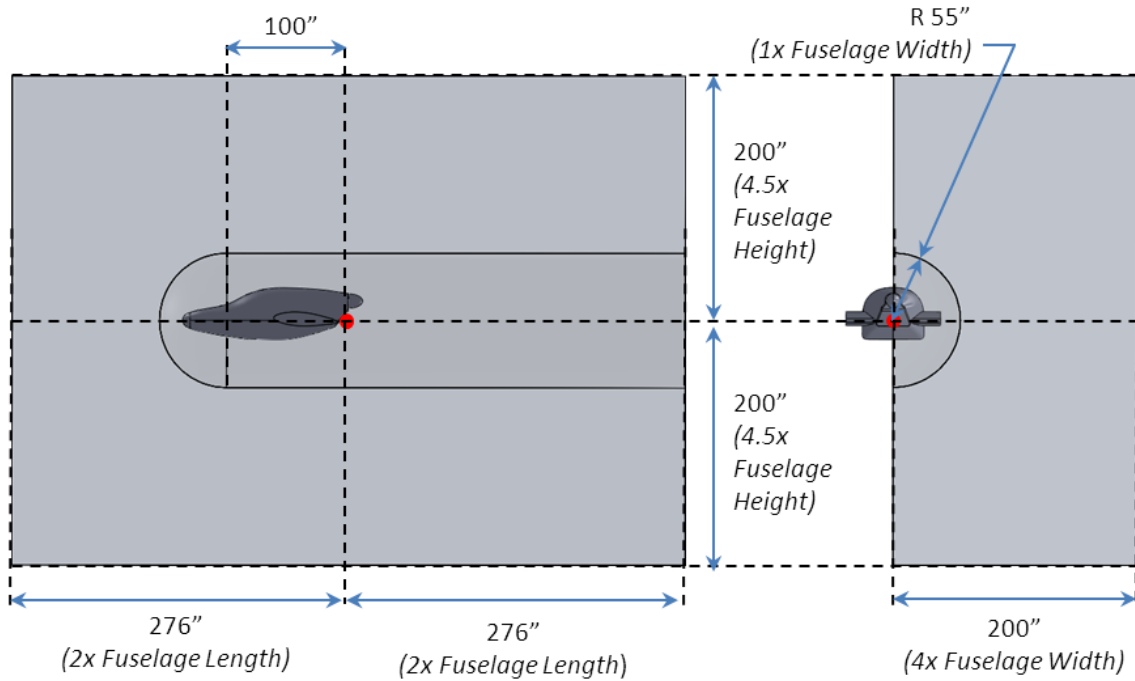


Figure 2-6: Computational Domain Dimensions

The final step before generating the mesh was to set-up the general mesh options. Most of the default settings for tetrahedral meshing were used with some exceptions. The options for advanced automatic sizing needed to be disabled since they could not function when manual sizing controls were used. The inflation options also needed to be manipulated. The Fluent application uses the term ‘inflation’ as the progressive scaling of cells in regions between elements of different sizes. It was found that the ‘Last Aspect Ratio’ setting for inflation provided the best transition from the fine mesh on the fuselage to the coarser setting on the wake-core and far-field faces. For reference and use in future applications, a step-by-step user guide is provided in Appendix A that walks through the process of meshing these computational domains in the Workbench mesh tool.

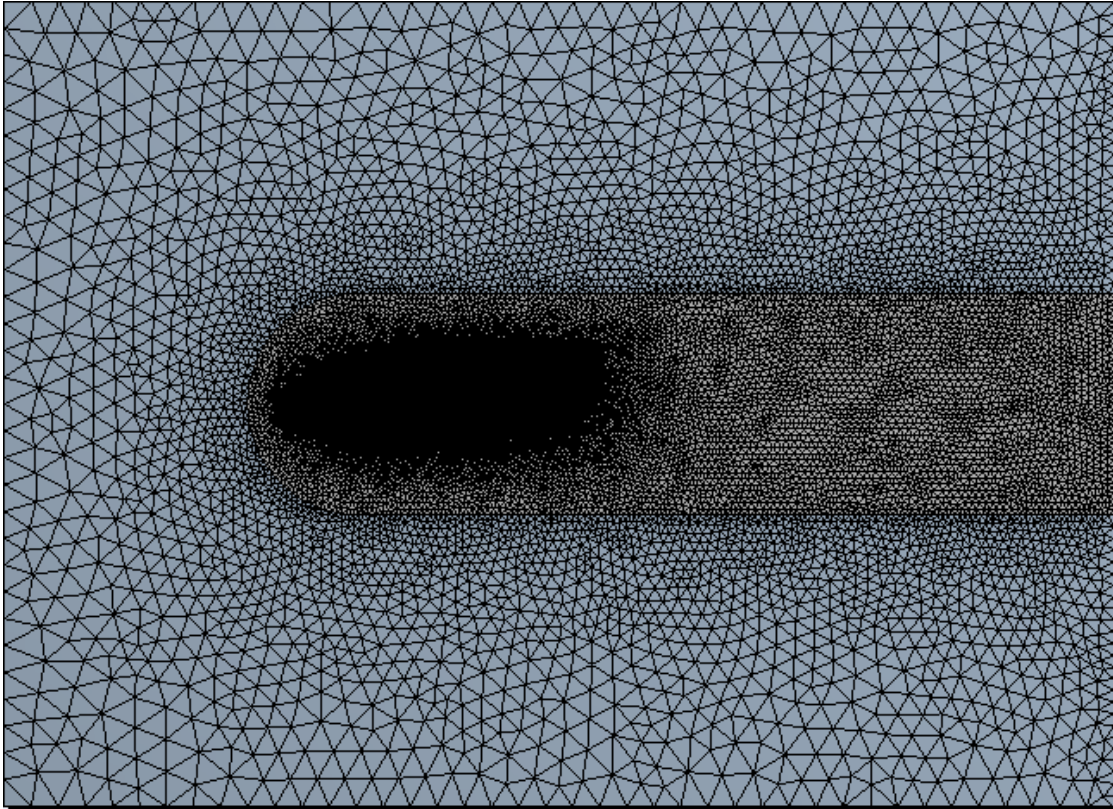


Figure 2-7: Vampire Fuselage CFD Mesh

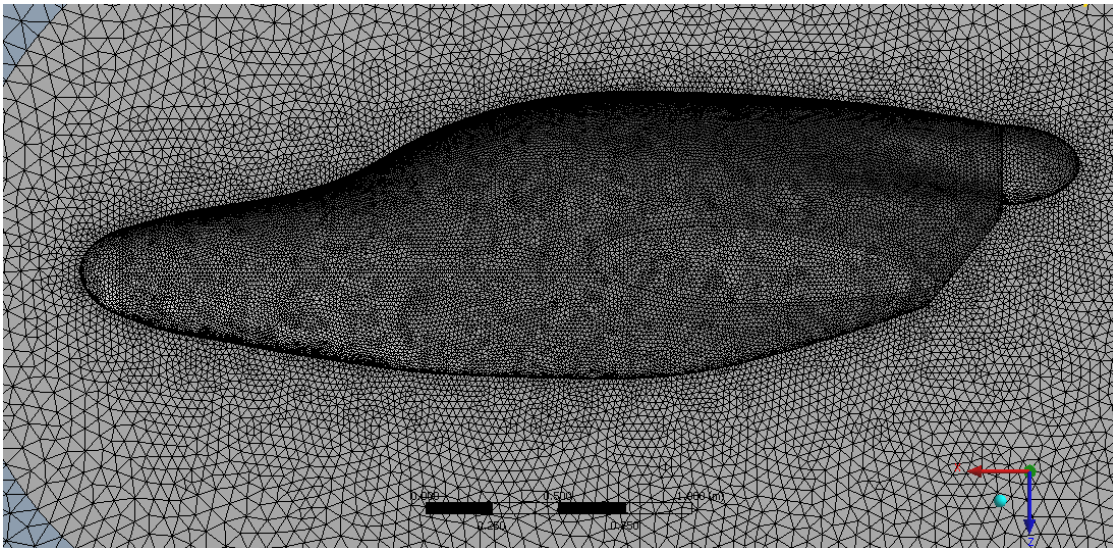


Figure 2-8: Vampire Fuselage CFD Mesh Close-Up

2.1.3 Fluent Set-Up

In CFD, the governing equation set that is chosen for the analysis will have the greatest effect on the final results. Fluent offers multiple aerodynamic models to choose from - both viscous and inviscid. Among them are the 1-equation Spalart-Allmaras (S-A) turbulence model, and higher order ones such as the 4-equation transition Shear Stress Transport (SST) model. Typically, CFD simulations are very computationally expensive and can take hours or even days to converge on a solution. It also stands to reason that higher order models with larger governing equation sets would require more computation time. Since the goal of this project work was to develop and implement a method that was both easy and fast to use, the S-A model was chosen. The choice was reinforced by previous studies that compared various turbulence models in CFD applications where it was found that the S-A model better matches the experimental wind-tunnel data for low angles of attack and cases where larger percentages of the reference chord had attached flow [3]. The SST model, on the other hand gave results that better matched wind tunnel test data for higher angles of attack where a higher percentage of the reference chord had separated flow [3]. In the internal flow modeling phase of the project, a comparison of the S-A and SST models was performed on a simulation of engine compartment internal flow (Figure 2-9).

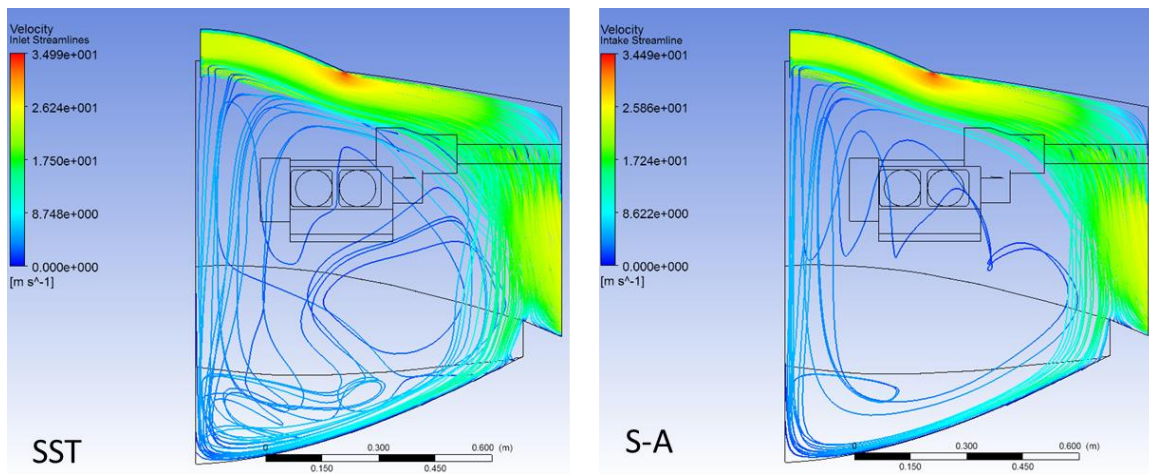


Figure 2-9: Turbulence Model Comparison

It was reasonable to assume that if there were significant differences in the results of the two aerodynamic models, the highly turbulent flow in the engine compartment would set them apart. Examining the flow visualizations in Figure 2-9, the two results are very similar. The only differences emerge in the streamlines of the near-stagnant flow. However, the SST simulation required a run time of 64 hours while the S-A model converged in 21 hours. As such, the nearly identical velocity and pressure results made the S-A model the clear choice.

In the set-up of the Fluent runs, most of the default settings for each option were used except for the mesh interfaces, boundary condition values, reference values, convergence criterion, and some solution controls. A detailed step-by-step process of the Fluent set-up is provided in Appendix A. It was important to define the mesh interface between the main computational domain and the wake-core bodies. If this step was not performed, then Fluent treated the wake-core as a solid body and the flow would completely bypass the aircraft model. As recommended in the ANSYS Fluent manual, the gradient solution method was set to ‘Green Gauss Node-Based’ as this was better suited to tetrahedral meshes [4]. Lift and drag monitors were set-up for the fuselage surfaces, the convergence criterion was set to $1e-6$ for all of the residuals, and the simulations were run for 3000 iterations. For fuselage analysis applications, Fluent reported typical computation times of about 20 hours.

2.2 Fuselage CFD Method Validation

To make sure that the mesh and Fluent solution set-up provided meaningful results, a benchmark case was run so that it could be compared to experimental wind tunnel data.

Using the method outlined in Section 2.1, a sphere of 62” diameter was modeled. This size was selected so that the reference chords of both the Vampire wing and the sphere were equal, thus producing meshes with the same element sizes and densities. Furthermore, spheres are well-studied blunt bodies for which experimental drag coefficient data is readily available. The mesh for the sphere test case is shown in Figure 2-10 on the following page.

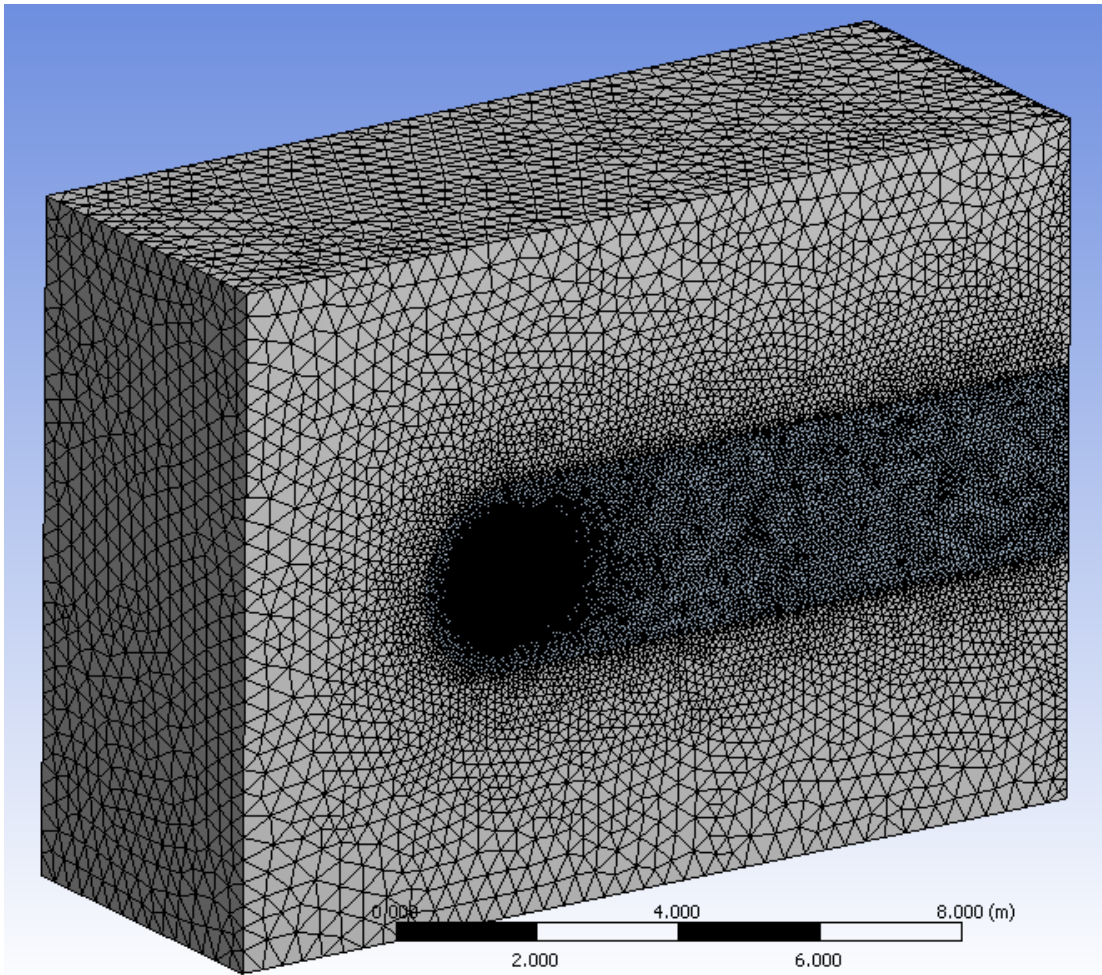


Figure 2-10: Sphere Drag Validation Mesh

The element size controls listed in Table 2-1 were used to mesh the sphere, and there were about 1.22 million elements. The element count for the sphere case was lower than the 1.5 million element limit due to geometric simplicity and lower surface area when compared to the Vampire fuselage. The free-stream conditions were set-up such that a Reynolds number of $1e6$ was attained for standard atmospheric conditions. This particular Reynolds number was chosen as it was the upper limit of the experimental data being referenced in NACA-TN-312 [5], which is the closest to the $6.78e6$ Reynolds number that the Vampire wing experiences when cruising at 120kts in standard atmospheric conditions at sea-level. The reference values for the test case are given in the following table.

Table 2-2: Sphere Reference Values

Parameter	Value
Reynolds Number	1e6
Chord (ft)	5.167
Area (ft ²)	20.97
Velocity (ft/s)	29.56
Dynamic Pressure (psf)	1.035

The Fluent simulation was set-up as described in Section 2.1 and 3000 solution iterations were commanded. The result was $C_d = 0.121$ and a $C_l = 0$. According to the NACA technical note, a sphere should have a C_d between 0.12 and 0.13, indicating that the Fluent CFD simulation and mesh provided an accurate and meaningful result. Thus, the mesh method and simulation set-up were validated. The following figures depict the rendering of the pressure and velocity results. Note that closer examination of the velocity rendering shows an asymmetric wake behind the sphere. This could likely be attributed to asymmetries in the tetrahedral mesh.

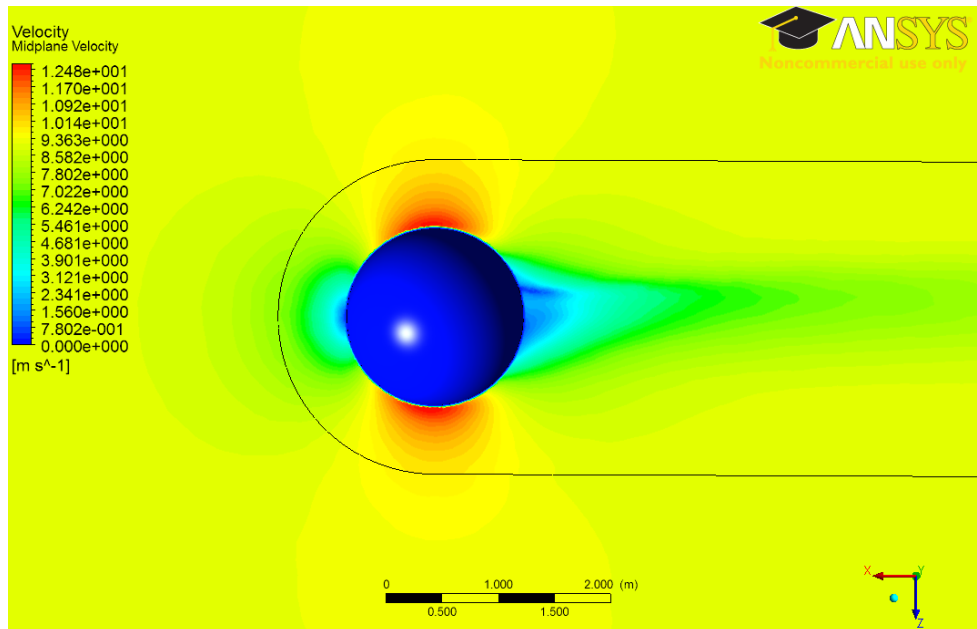


Figure 2-11: Sphere Drag Validation Velocity Rendering

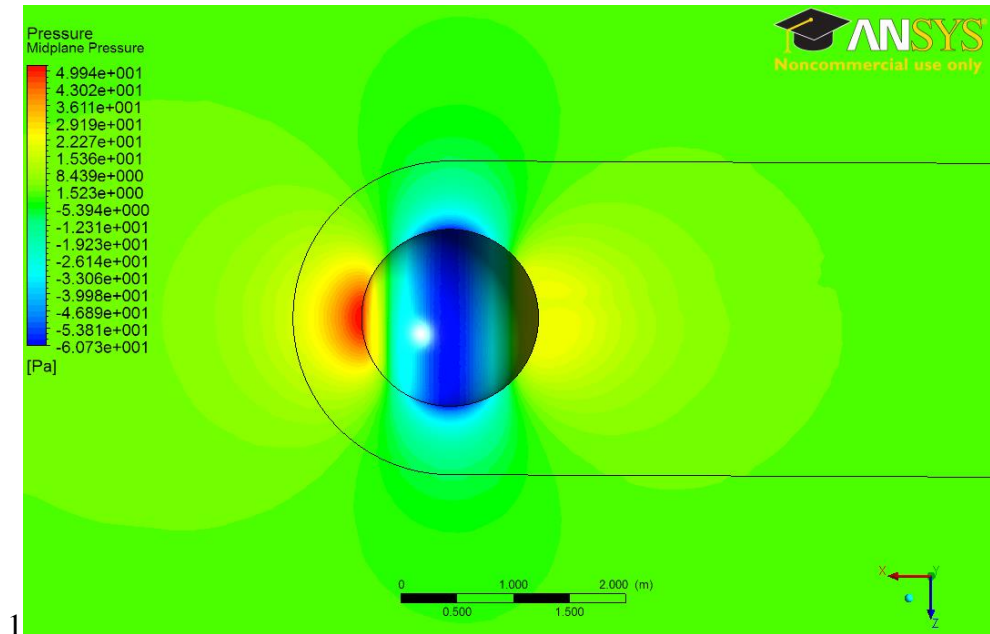


Figure 2-12: Sphere Drag Validation Pressure Rendering

2.3 CFD for Internal Flow Modeling

The flow analysis within the engine compartment was more simple to mesh and set-up than the external fuselage flow models. Again, the computational domain and internal components were modeled in SolidWorks and arranged in an assembly. The ANSYS 13 Workbench Design Modeler tool was used to volume-subtract the internal components from the fluid volume before meshing in the Workbench mesh tool. This section provides more detail on the CAD modeling and meshing process for internal flow applications.

2.3.1 CAD Modeling

In the case of the Vampire, the engine compartment is defined by the volume contained within the fuselage aft of the firewall. This volume could be easily modeled using the full fuselage CAD models that were also used for the external fuselage drag analysis. In the SolidWorks part file, planes were defined along the firewall and aircraft centerline, and the excess volume was cut away from the fuselage as shown in the following figure. The fuselage skin thickness was not subtracted from the fluid volume and was omitted to simplify

the modeling process. This was also done because the skin thickness would not be known until detailed structural analysis is performed.

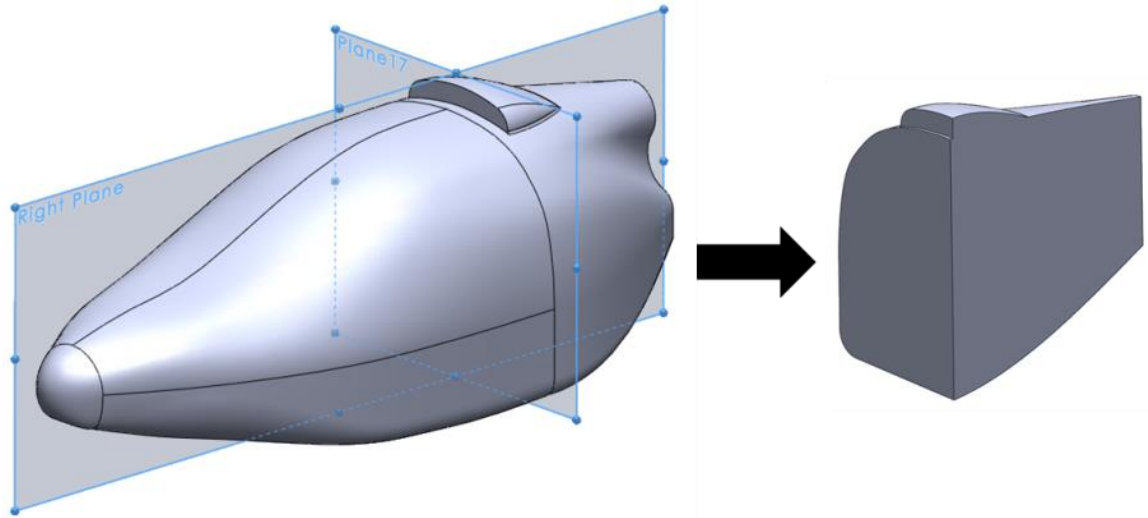


Figure 2-13: Creating the Internal Flow Computational Domain

In Figure 2-13, an example re-designed Vampire fuselage with a single roof-mounted intake scoop is shown. The next step was to arrange internal components such as the engine, wing structure, and baffles in a SolidWorks assembly as shown in Figure 2-16 on the left. The engine, driveshaft, and wing analogs were modeled as solids and positioned in the assembly in their respective locations. Note that the fluid volume model is also a solid, but it is shown to be transparent for clarity. The assembly was then exported to the ANSYS Workbench design modeler where the ‘boolean subtract’ feature was used to remove the volumes of the wing and engine from the computational domain as shown in Figure 2-14 on the next page.

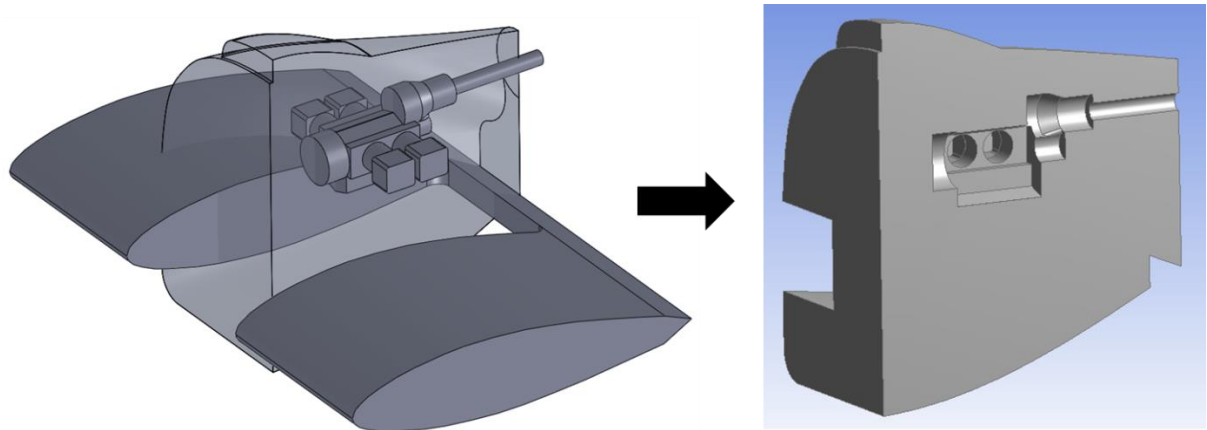


Figure 2-14: Internal Flow Model Assembly

2.3.2 Meshing

Since the internal flow direction is mostly unknown in the engine compartment, all regions of the computational domain were treated equally. This greatly simplified the meshing process as this allowed use of the automatic meshing features in the Workbench mesh tool by defining a constant element size throughout the domain. Again, this was a trial-and-error process where the goal was to find an element size that provided the finest mesh while complying with the 1.5 million element limit. An example internal flow mesh is shown in Figure 2-15 where the element size was set to 0.0129m. Since the internal flow computational domain was not comprised of multiple volumes to control mesh inflation, defining the named selections was also simplified. For these cases, the only named selections required were ‘inlet’, ‘outlet’, and ‘symmetry’. All other faces were left unnamed so that Fluent automatically assigns the ‘wall’ boundary condition. Note that the Fluent simulation set-up and solver settings were identical to the method for external fuselage drag analysis.

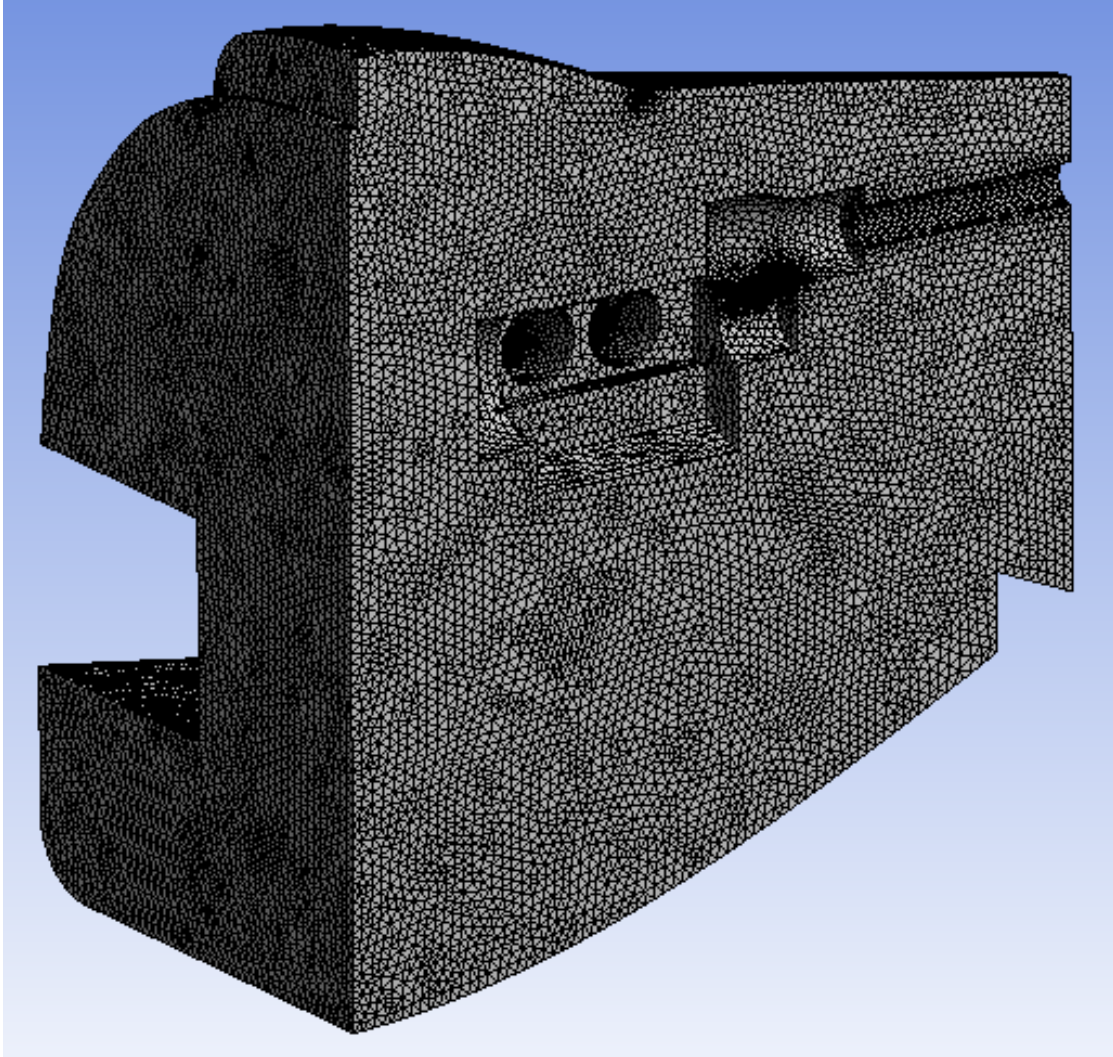


Figure 2-15: Example Internal Flow Mesh

3 Fuselage Design

Once the CFD drag analysis method was established and verified, the next phase of the project could begin: the re-design of the Vampire fuselage. As mentioned in Section 1, the existing Vampire prototype was designed for two-person side-by-side seating with a distinctive high visibility cockpit with gull wing doors. LSA America indicated that they favored the forward fuselage design as it gives the aircraft a good aesthetic profile that sets it apart from any other aircraft in the LSA category. Since the largest drag contributor was the aft face of the fuselage, it was decided that only the fuselage portion aft of the firewall would be modified. The goals for the re-design included the following:

- Reduce fuselage drag.
- Maintain overall aircraft aesthetics.
- Ease the manufacturing process by designing the aft-fuselage such that the existing fuselage molds may be used with some modifications.
- Make provisions for ample engine cooling.
- Shorten the aft fuselage as much as is practically possible so that the engine extension shaft may be shortened or eliminated.

First, the prototype fuselage was analyzed for drag using the CFD method outlined in section 2. This set the baseline drag coefficient for which the new designs would be compared. Then new designs were created in SolidWorks and analyzed in Fluent. There were three designs that had a lower drag coefficient than the baseline, and one was selected based on the primary criteria listed above.

3.1 Establishing the Baseline

When analyzing complex shapes for lift and drag, it is important to take into account any other geometric or design features that would affect the flow around the object, and thus the results. Since the Vampire is a low-wing aircraft, the low pressure region over the NACA 63-218 wing with $+4^\circ$ of incidence causes adverse pressure gradients that would affect flow separation on the aft fuselage. To account for this, it was decided that the fuselage models would incorporate the portion of the wing located between the two tail booms. The 11.8" x 11.4" (30cm x 29 cm) spinner also acts to streamline the flow aft of the fuselage, so it was also incorporated to the solid model. For the purpose of the fuselage design and analysis, the ram air intakes were neglected. This was primarily because they would add complexity to the model where flow into and out of the fuselage would need to be accounted for to obtain accurate results. The following figure shows the major dimensions for the baseline fuselage:

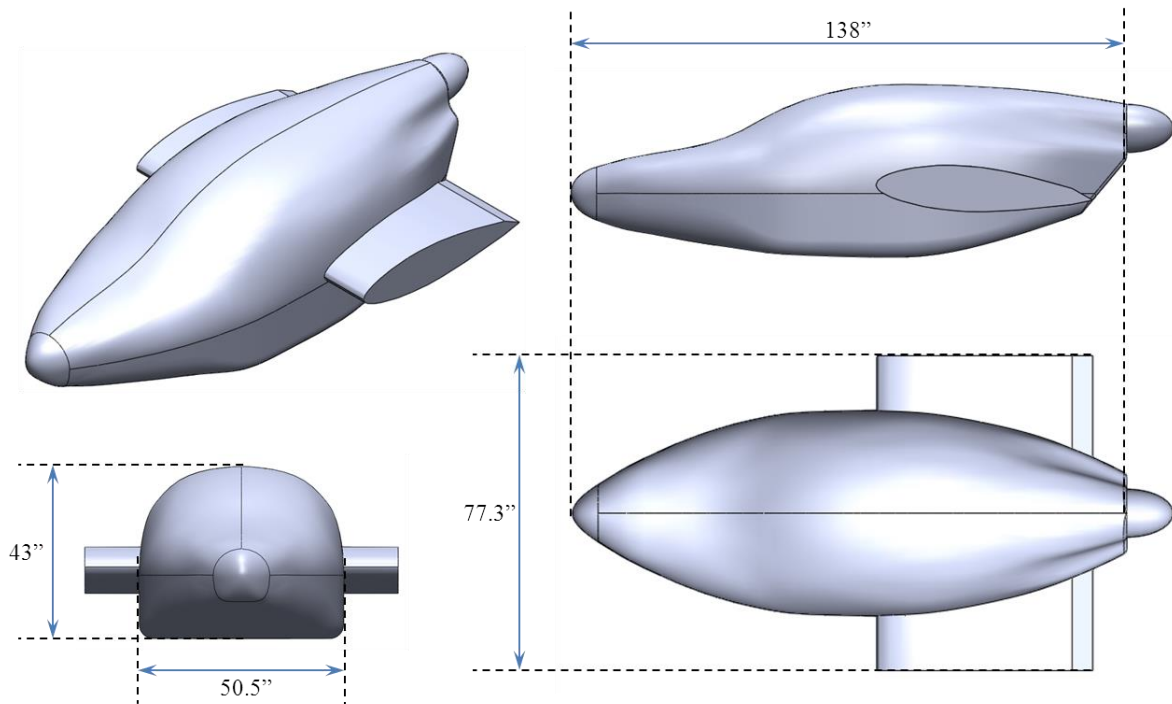


Figure 3-1: Baseline Fuselage Major Dimensions

Figures 2-10 and 2-11 show the mesh for the baseline fuselage which had 1.48 million elements. The following table lists the reference values used to set up the boundary and flow conditions for the Fluent analysis. Note that the analysis was performed at the maximum cruising speed for the Light Sport category of 120kts with zero degrees of fuselage pitch. Standard day sea-level pressure, density, and temperature were used.

Table 3-1: Baseline Fuselage Reference Values

Parameter	Value
Chord (ft)	5.167
Area (ft ²)	134.3
Velocity (ft/s)	202.5
Dynamic Pressure (fps)	47.99
Reynolds Number	6.868e6

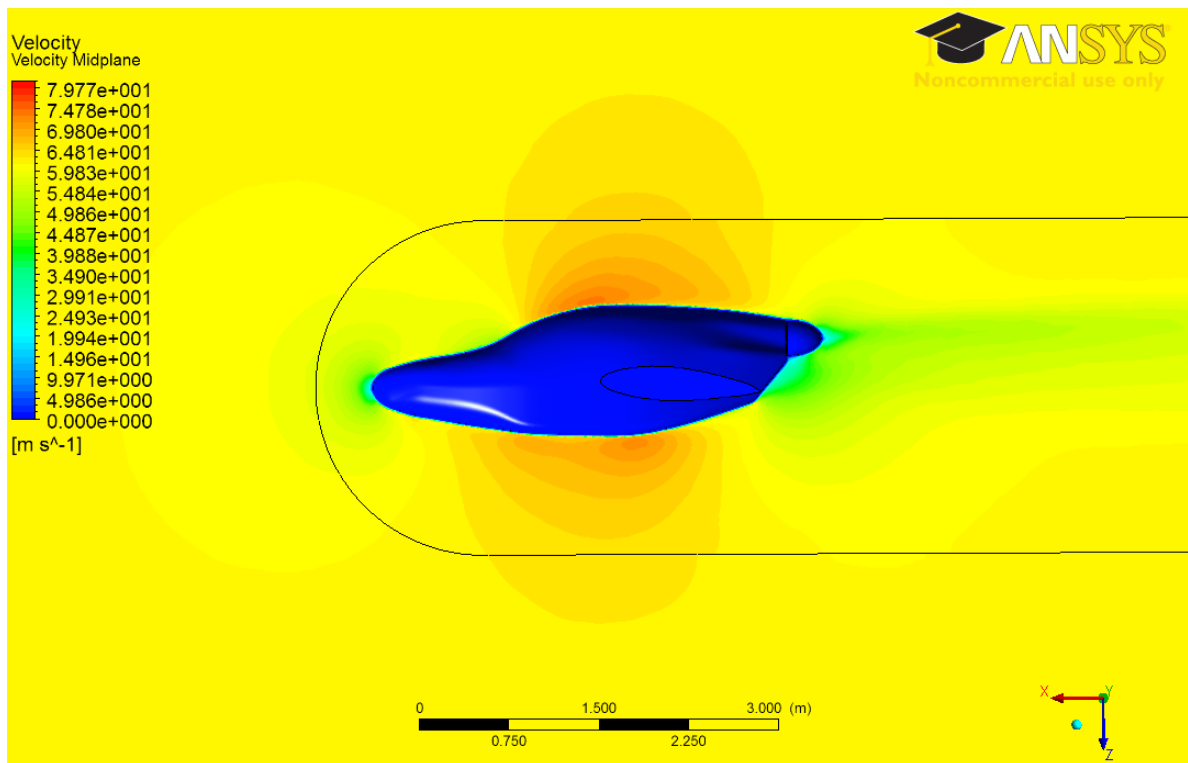


Figure 3-2: Baseline Fuselage Velocity Contours (120kts)

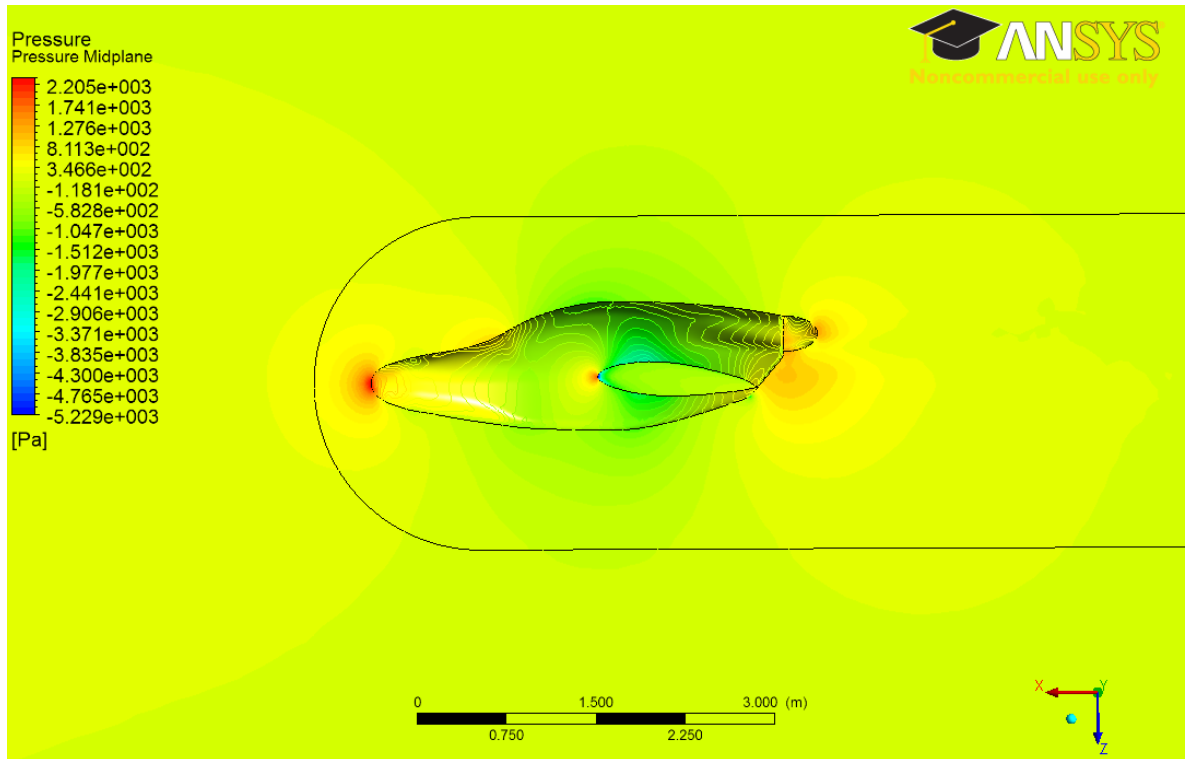


Figure 3-3: Baseline Fuselage Pressure Contours (120kts)

The Fluent solution gave a drag coefficient of $C_d = 0.0150$. A closer examination of Figure 3-2 showed a large region of separation where the fuselage swept upwards. According to the Sadler CAD files, the angle on that face is about 50° , and this makes it a primary contributor of pressure drag on the aircraft. However, it should be noted that the effects of induced flow from the pusher-propeller are not being modeled although these effects generally help reduce adverse pressure gradients and thus reduce drag. On the other hand, modeling propeller effects is complicated in CFD set-ups, and it would add a level of complexity that is beyond the scope of this project. Instead, it was decided that all fuselage configurations for the Vampire project would be modeled without propeller effects as the results still give a relative drag comparison between configurations.

3.2 Dimension Constraints

Before reconfiguration of the Vampire fuselage could begin, all of the design and dimensional constraints needed to be identified. These constraints were dictated by aspects such as internal structures, the engine, and fuselage wrapping around the desired seating layout. To reduce the pressure drag on the fuselage, the first goal was to reduce any up-sweep angles on the fuselage below 30° . According to Raymer [6], this should be the maximum angle that pusher-configuration fuselages have before encountering large flow separation problems. Reducing the overall length of the fuselage would also accomplish a reduction in skin-friction drag from having less wetted area. As such, it was necessary to determine how much the fuselage length could be reduced. The answer came from a closer inspection of the internal wing structure.

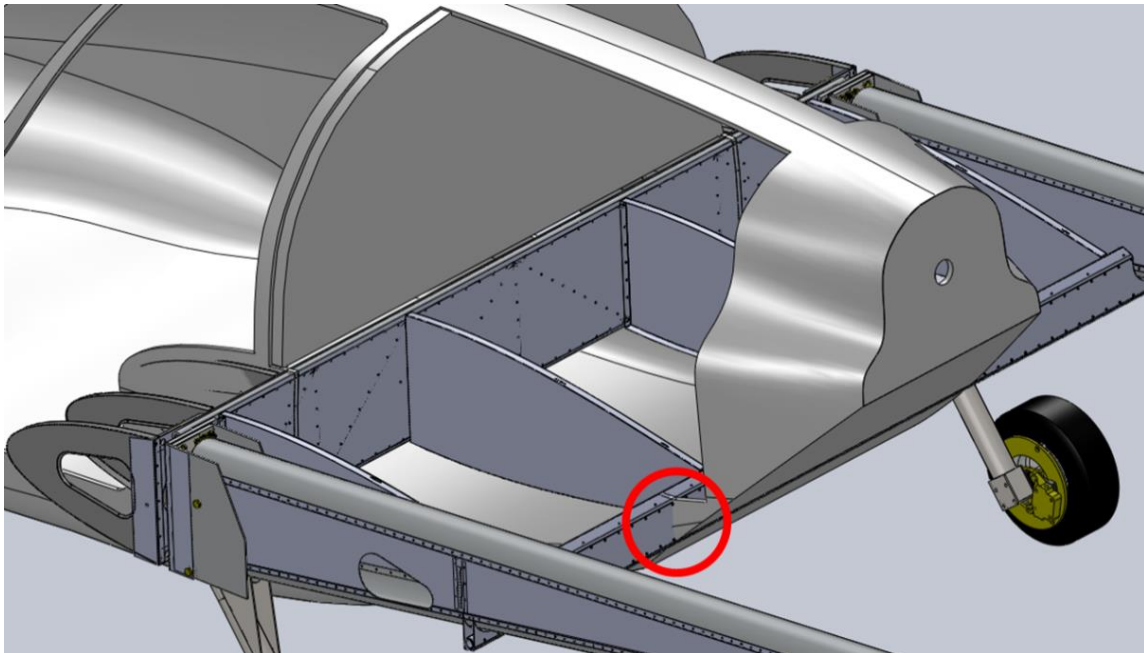


Figure 3-4: Internal Wing Structure

As shown in Figure 3-4, the main spar mounted directly to the firewall, and as indicated by the red circle, the aft spar was located very close to the aft face of the fuselage. Because of this feature, the wing portion between the tail-booms had a shorter chord since the full 62” design chord protruded beyond the aft face of the fuselage. To work around this, the prototype was manufactured such that the airfoil profile was continued to the wing’s aft spar, and then a trailing edge wedge was installed from the aft spar up to the aft face of the fuselage as seen in the following figure.

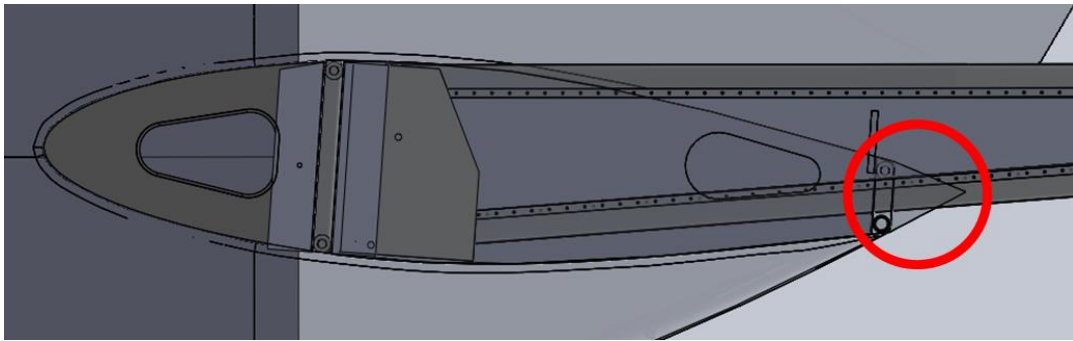


Figure 3-5: Wing Trailing Edge Detail

The reduced chord for this section of the wing was 54.9”. Without the trailing edge wedge, the remaining chord was 47.8”. An option was considered where the trailing edge wedge would be omitted to simplify the manufacturing process. However, an investigation into the truncating an airfoil indicated that there would be a substantial drag penalty. The following equation from Hoerner [7] was used:

$$\Delta C_d = \frac{0.34}{\sqrt[3]{C_{d,0}}} \left(\frac{\Delta c}{c_d} \right)^{\frac{4}{3}} \quad \text{Eq. 3-1}$$

ΔC_d is the change in drag coefficient, $C_{d,0}$ is the baseline drag coefficient for the airfoil, Δc is the percent change in chord due to the truncation, and c_d is the baseline airfoil chord. Using XFOil, a well-known two-dimensional panel code for analyzing airfoils, the NACA 63-218 has a zero-alpha drag coefficient of 0.0033 for a Reynolds number of 6.87e6. Substituting

this value along with the chord truncation of 22.8%, the equation indicated that the drag coefficient would increase by 0.32. This is a substantial increase in drag, and resulted in the decision to retain a trailing edge wedge. Further investigation was made to determine if there is a wedge angle that minimizes the drag of the modified airfoil section. However, experimental data indicated that the drag as a function of wedge angle monotonically increases from its minimum at zero degrees wedge angle - which is basically a flat plate [8]. It was decided that the trailing edge wedge would extend 4" aft of the aft spar which was also about 4" in height. In all, this sets the minimum fuselage length – not including the spinner – to 126".

Reducing the base area of a fuselage will also reduce the drag of a fuselage. This is typically accomplished by closing the fuselage to a point much the same way that an airfoil's upper and lower camber converge on a trailing edge. Of course, there are several factors that limit the aft fuselage closure. For pusher configurations, there must be ample room to fit the engine, and in this particular case the fuselage must accommodate two people in a side-by-side seating arrangement so the cross section must not be too narrow. As shown in Figure 3-6, the cabin cross section could not be more tightly wrapped at the firewall without making the cabin cramped; thus, the cross-section at the firewall would not be modified in the re-design. Additionally, the areas indicated in light blue represented the location of the fuel tanks. These tanks were sheeted and sealed portions of the wing with an open bay of width 24.5" situated between them. So as to not expose this open area, the fuselage re-design was constrained to a minimum fuselage aft-face width of 24.5".

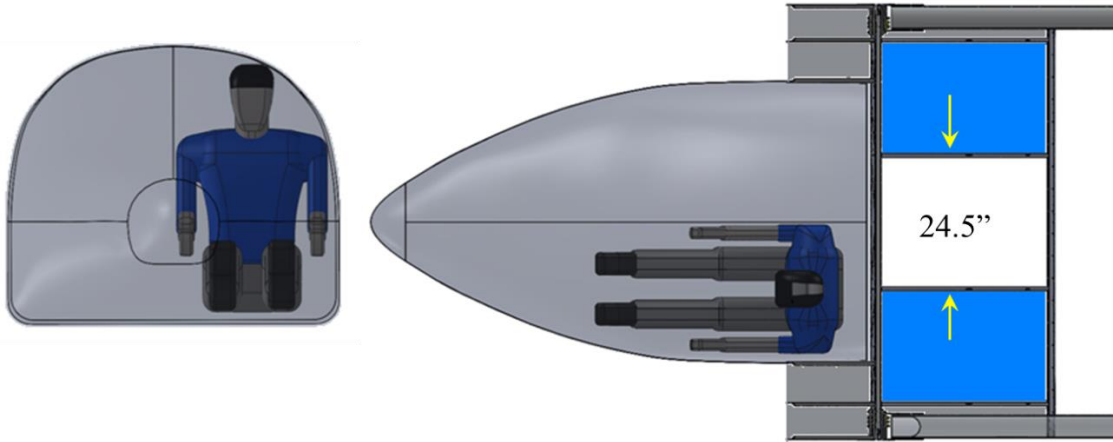


Figure 3-6: Width Constraints

The last geometric constraint on the re-design was the spinner. Since a new engine – the Rotax 912 ULS – was to be integrated into the new fuselage, the spinner dimensions needed to be updated. The new spinner was 9.84” in diameter and 9.44” in length (25cm x 24cm).

3.3 New Design Configurations

Using the constraints established in Section 3.2, new fuselage configurations were developed and tested in Fluent. To keep the modeling simple, a two-profile loft modeling approach was used. This involved truncating the original fuselage model at the firewall since the profile forward of the firewall was to remain unchanged from the prototype. A sketch plane was defined at the aft limit of fuselage, and the aft-most cross-sections were drawn on the plane. The loft could then be created by selecting the firewall face and extruding it to the aft-most cross-section. Since they were not present on the prototype fuselage, half-inch radius fillets were also added at the wing-fuselage interfaces to reduce interference drag. The new fuselage configurations all featured non-sloped blunt aft faces. Normally, this would contribute more base drag than the 50° sloped face on the baseline fuselage. However, the blunt face was intended to be cut out of the fuselage so that it functioned as a large cooling outlet. The idea is that ram intake air would exit through this outlet, mix with the free-stream, and thus reduce pressure drag.

A total of three configurations, shown in Figure 3-7, were presented to LSA America where a final selection was made based on drag improvement, manufacturability, and aesthetics. Table 3-2 compiles the data comparing the configurations to the base line. This sub-section details the three configurations and their analysis. Note that equation 3-2 was used to calculate power required to propel the fuselage and partial wing section at a velocity of 120kts:

$$P_R = 0.5\rho V^3 S C_d * \frac{1}{550} \frac{hp}{ft*lb/s} \quad \text{Eq. 3-2}$$

Table 3-2: New Fuselage Configuration Comparison

Parameter	Baseline	V1	V2	V3
C_d	0.0150	0.0139	0.0134	0.0132
Fuselage Length (in)	136	126	126	126
Wetted Area (in ²)	15,807	14,976	15,113	15,001
Bluff Area (in ²)	439	228	187	187
Max Aft Closure Angle (deg)	50	32	38	31
% Drag Reduction	--	6.9	10.4	11.5
Power Required (hp)	36.1	33.4	32.2	31.7

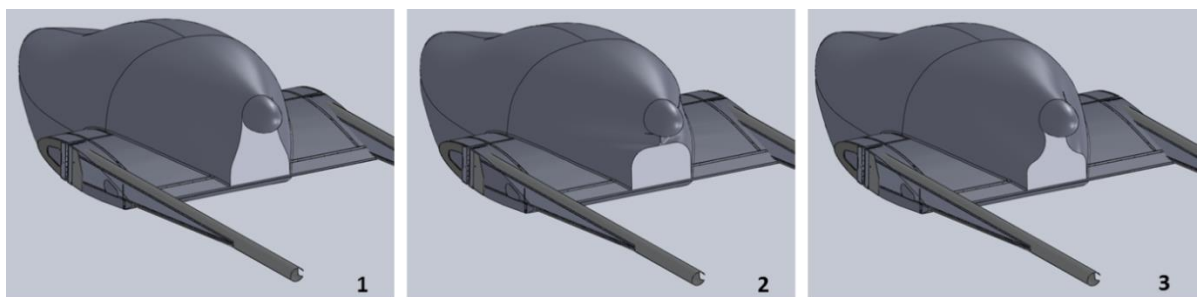


Figure 3-7: New Fuselage Configuration Options

3.3.1 Version 1

The configuration labeled '1' in Figure 3-7 was the first iteration of the re-design. It conformed to the 126" length and 24.5" aft-width constraint without modifying the cross-section at the fire-wall. The spinner was located in a high-mount position to provide additional propeller clearance and to keep the engine near the roof of the engine compartment to increase the effectiveness of a roof-mounted cooling intake scoop. The aft profile was shaped such that the lower section, which was constrained to the 24.5" minimum width, tangentially blended to the diameter of the spinner cone by means of an s-shaped curve. This is seen more clearly in the following figure.

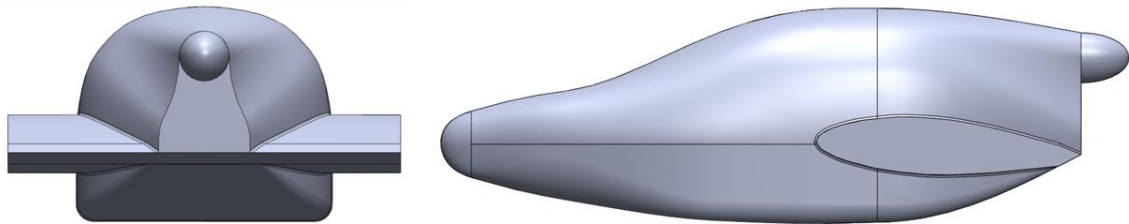


Figure 3-8: Rear and Side View for New Fuselage v1

The reference values for the Fluent analysis were the same as those used in Table 3-1. The drag coefficient was 0.0139 representing a drag reduction of 6.9%. Although the bluff face area of this configuration was 228 in², the drag reduction could be attributed to lower skin-friction drag as a result of reduced wetted area. The reduction in the maximum closure angle also assisted in pressure recovery. The CFD renderings for this intermediate configuration can be found in Appendix B.

3.3.2 Version 2

To further reduce the base drag, the outlet area needed to be reduced. According to Raymer, the outlet for engine cooling should be about 39% to 65% of the engine's frontal area [9]. For the Rotax 912 ULS, this area is about 2 ft² which placed the first iteration's outlet area at 79% engine frontal area. Considering that pusher configurations have inherent cooling challenges, it was decided that the target outlet area would be at the upper range of 65%. An attempt was also made to close a portion of the aft fuselage to a point. This was done by 'pinching' the loft below the spinner and extending it just low enough to accommodate a rectangular outlet of area 187 in². This is depicted in Figure 3-9:

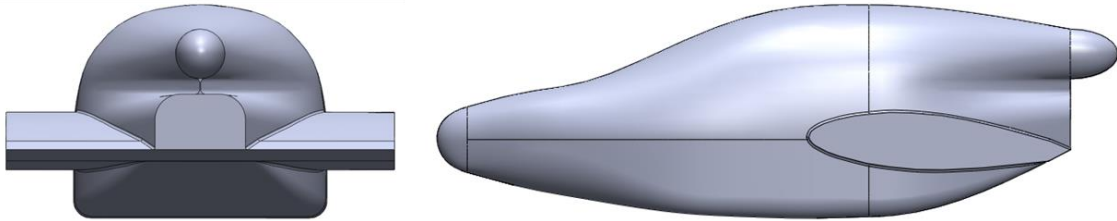


Figure 3-9: Rear and Side View for New Fuselage v2

References parameters from Table 3-1 were used for Fluent analysis, and the resulting drag coefficient was 0.0134 representing a drag reduction of 10.4% over baseline. This further improved drag value was attributed to the reduction of the engine compartment outlet area. The CFD renderings for this configuration are available in Appendix B.

Although the drag reduction compared to the baseline was a significant improvement, there were some aspects of the second intermediate configuration that made it unsuitable as the final design. Firstly, the complete closure of the fuselage between the spinner and cooling outlet would complicate the manufacturing process; there is no clear location for a mold parting plane which means that when the composite layup was performed, it would be more difficult to remove the part once it was cured. Secondly, this configuration is not as

aesthetically pleasing and the geometric cues of the aft fuselage do not agree with the forward fuselage. This necessitated another re-configuration.

3.3.3 Version 3 - Final

The third and final configuration was influenced by the successes of the first and second intermediate designs. Instead of pinching the fuselage closed below the spinner, like in version 2, the target outlet area of 187 in^2 would instead be accomplished by forming an s-curve from the base of the aft profile upwards toward the spinner like in version 1. The result was the final configuration shown below and the CFD renderings of the simulation are given in the figures on the next page.

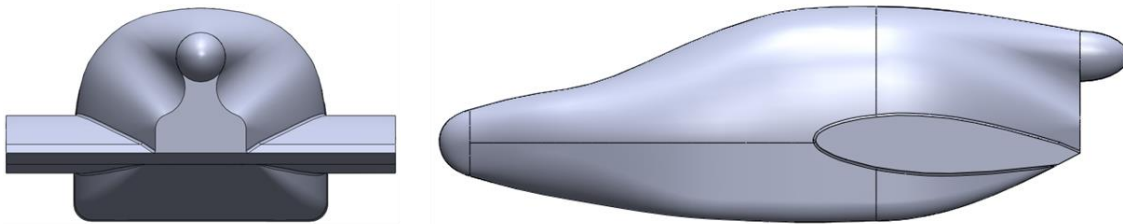


Figure 3-10: Rear and Side View for Final Configuration

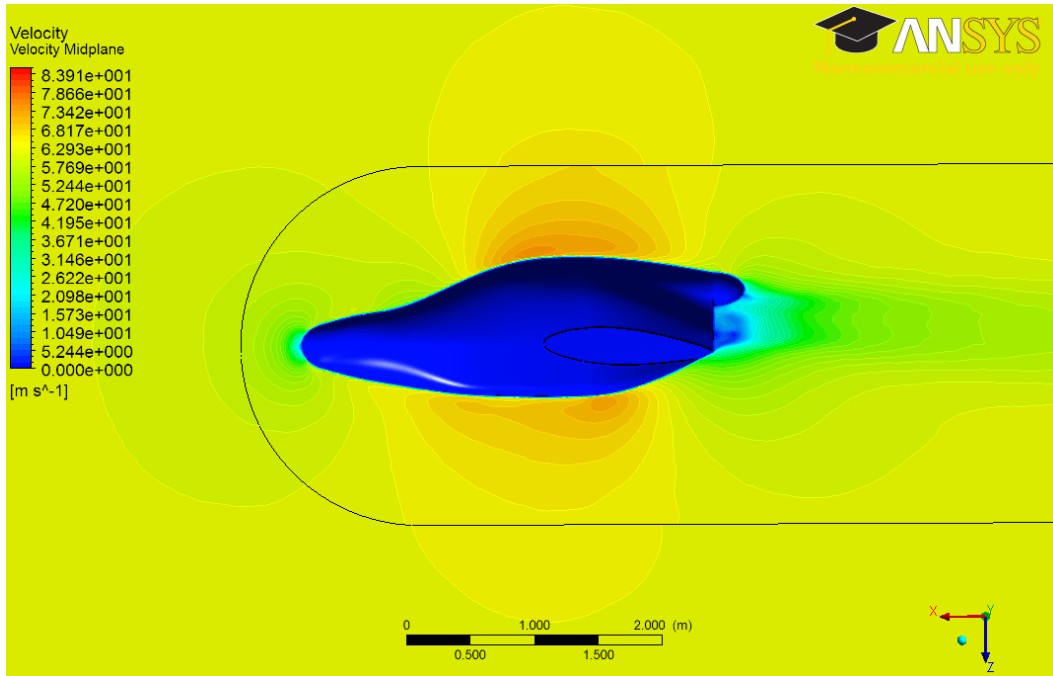


Figure 3-11: New Fuselage CFD Velocity Contours

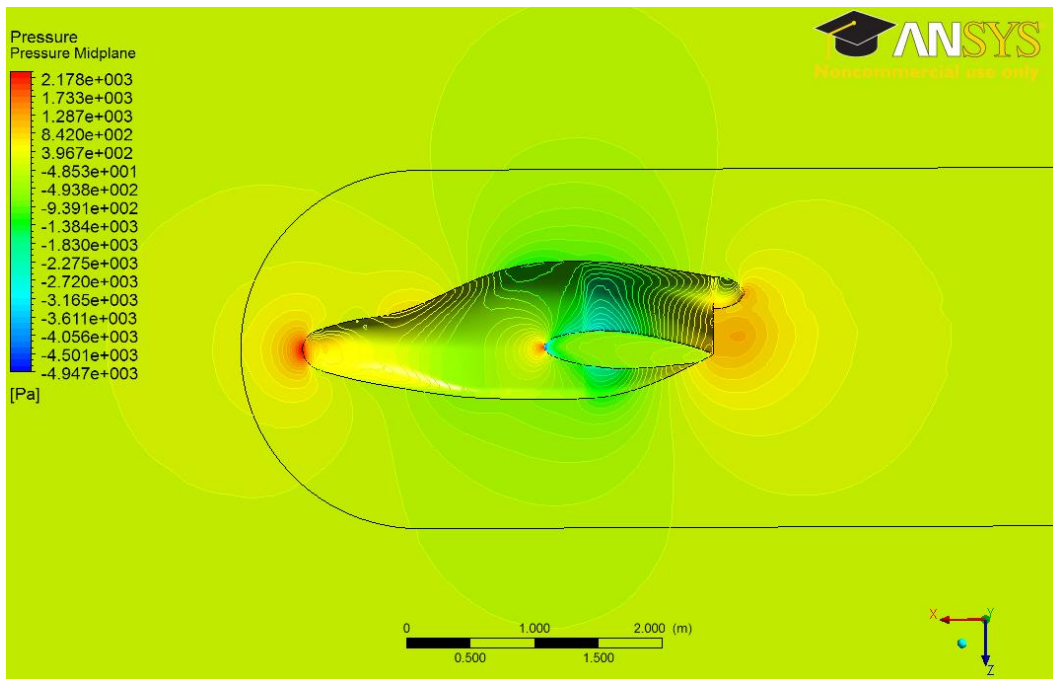


Figure 3-12: New Fuselage CFD Pressure Contours

The third configuration had a drag coefficient of 0.0132 – an 11.5% reduction when compared to the baseline. The drag was slightly lower than the second iteration despite having slightly more wetted area; this was likely due to having less interference drag in the absence of the aft fuselage closure. Comparing Figure 3-12 to Figure 3-3, the new fuselage shows improved pressure recovery over the baseline fuselage as evidenced by the pressure contours. In Figure 3-3, the contours extend outside of the wake-core, whereas in Figure 3-12 the pressure recovers within the wake-core volume. Another feature to note is the stagnation region about the new fuselage’s cooling outlet. Since it was modeled as a closed solid, the simulation shows that this causes flow separation. However, despite the bluff aft face, the drag value for the new fuselage configuration is significantly lower than the baseline fuselage. This can be attributed to the improved streamlining of the aft fuselage along with a reduction in wetted area. It was important to keep in mind that the actual drag coefficient would decrease if cooling flow exiting the outlet were modeled. After consulting LSA America, it was agreed that the third iteration of the fuselage design was satisfactory for its aesthetics, significant drag reduction, and that it could be manufactured by adding plugs to the existing fuselage molds.

4 Engine Integration

The positioning and cooling provisions for the engine could be performed after the new fuselage design was determined. As requested by LSA America, a Rotax 912 ULS, which is a 4-stroke 4-cylinder horizontally opposed small aircraft engine, was to be integrated into the Vampire airframe. The cylinder bodies were cooled by ram air, and it had radiators for cylinder head and oil cooling. LSA America was unable to provide dimensions and specifications for the engine mount and exhaust system that they use on the Allegro, so integration work with the Vampire was done assuming the stock Rotax engine mount and exhaust components as detailed in the engine's installation manual [10]. All integration work was performed using a SolidWorks assembly and an engineering model of the Rotax 912 ULS. For cooling, a primary intake scoop was designed and positioned on the roof of the fuselage to cool the engine and provide it with intake air for combustion. A secondary intake scoop was positioned on the belly of the fuselage to allow for some cooling of the exhaust system components and to assist in directing the ram air from the upper scoop out through the engine compartment's outlet. Several baffles were required to direct the ram air to serve these functions. This section will detail the engine positioning, cooling intakes, and baffle designs.

4.1 Engine Positioning

To integrate the Rotax 912 ULS engine, an engineering CAD model, shown in Figure 4-1, was used [11]. Although this model did not include every wire and hose, it modeled the major components necessary for proper positioning and preliminary integration work.

Locating the engine in the engine compartment was constrained by the position of the spinner and the dimensions of the engine suspension frame. The engine's output shaft was aligned such that it was concentric with the spinner. The Rotax installation manual [10] provided coordinates for the stock engine suspension frame, and when modeled in SolidWorks, it

showed that there was about 1” of clearance between the air box and front face of the firewall. The location of the engine as installed in the new Vampire fuselage is depicted in Figure 4-2.

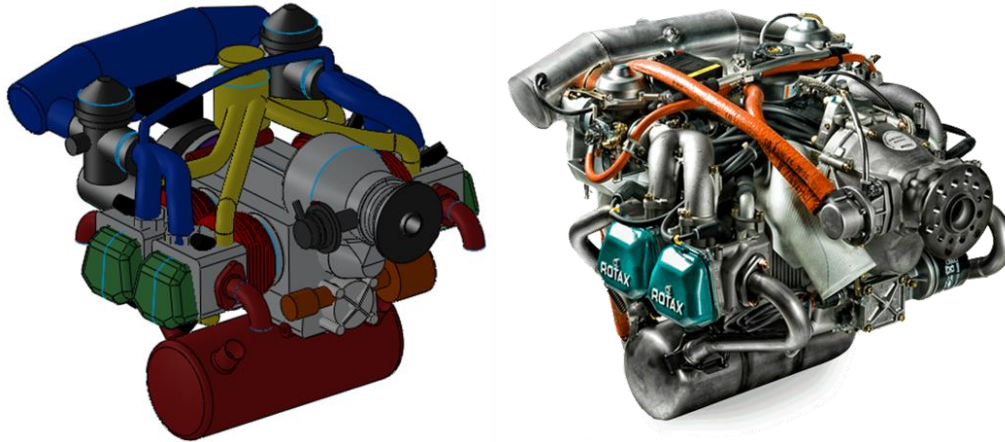


Figure 4-1: Rotax 912 ULS Engine (right) and CAD Model (left)

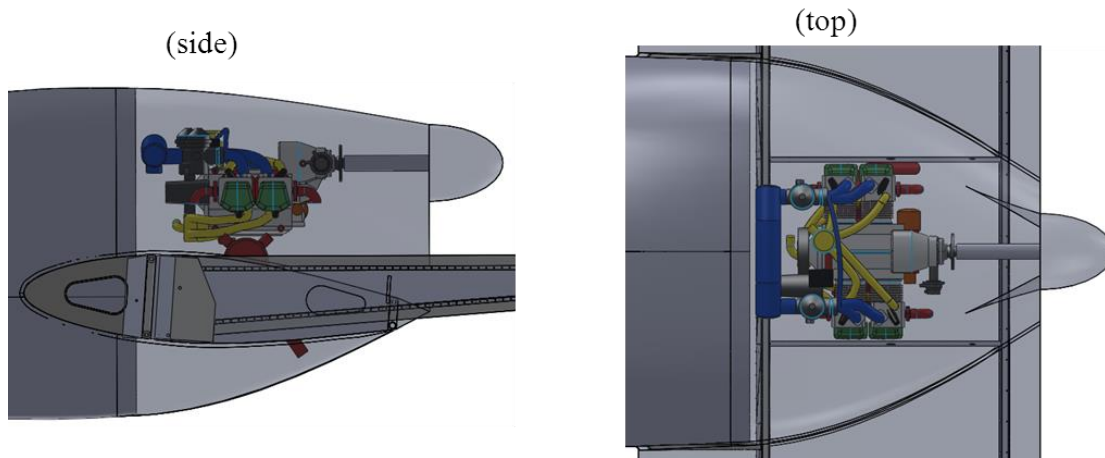


Figure 4-2: Engine Position in Engine Compartment

Although the new fuselage is shorter than the prototype fuselage, the Rotax 912 ULS still required an extension shaft to reach the spinner. The extension shaft was 10.9” in length. It should be noted that the shaft length will need to be revised if spatial integration is re-iterated using the Allegro engine suspension frame as originally intended by LSA America.

Furthermore, the stock exhaust pipe was not long enough to vent exhaust outside the engine compartment. According to the spatial integration model, an extension of at least 2.75” would be required.

4.2 Cooling Airflow

The guidance of the interior cooling airflow followed a build-up process. Beginning with the engine bay fluid volume, the positioned engine, extension shaft, and internal wing structure, Fluent simulations were set-up using the method detailed in Section 2.3. Since the aircraft’s take-off run is the most cooling-critical phase of flight where high throttle settings and low airspeeds are experienced, the flow conditions at takeoff rotation were simulated. The Sadler Aircraft design files indicated that the Vampire had a stall speed in the clean (no flaps) configuration of 45 kts. Takeoff rotation speed is typically specified as $1.1 V_{\text{stall}}$ [12], and this gave the free-stream a velocity 49 kts (82.3 ft/s).

The first step was to design an air intake scoop positioned on the roof of the fuselage. Scoops on the side of the fuselage and on its belly were also considered, but the side-mounted configuration was ruled out due to the width of the fuselage compared to the narrow engine. The belly-mounted location was ruled out to avoid Foreign Object Debris (FOD) ingestion. As a rule of thumb, the air intake area is sized to about 30% to 50% of the engine frontal area [9]. Initial intake scoop geometries aimed for the upper limit of 50%, which for the Rotax 912 ULS is about 144in^2 . However, these intakes proved to be very large and they drastically affected the aesthetics of the aircraft and would likely negate any drag benefits gained from the new fuselage design. The final intake scoop had an area of about 69in^2 , which is about 34% of the engine frontal area and was still within the bounds of the recommended intake sizing. No attempt at optimizing the air intake scoop was made. Instead, it was shaped to match the contours of the aircraft in a ‘looks-about-right’ fashion. The upper intake scoop is depicted in Figure 4-3. The intake scoop was about 22.9” wide and 3.25” in height. It extended 16” aft where it narrowed to a width of 13.5”. To mitigate interference drag, there was a 0.5” fillet along the sides and back of the scoop to blend it to the fuselage.

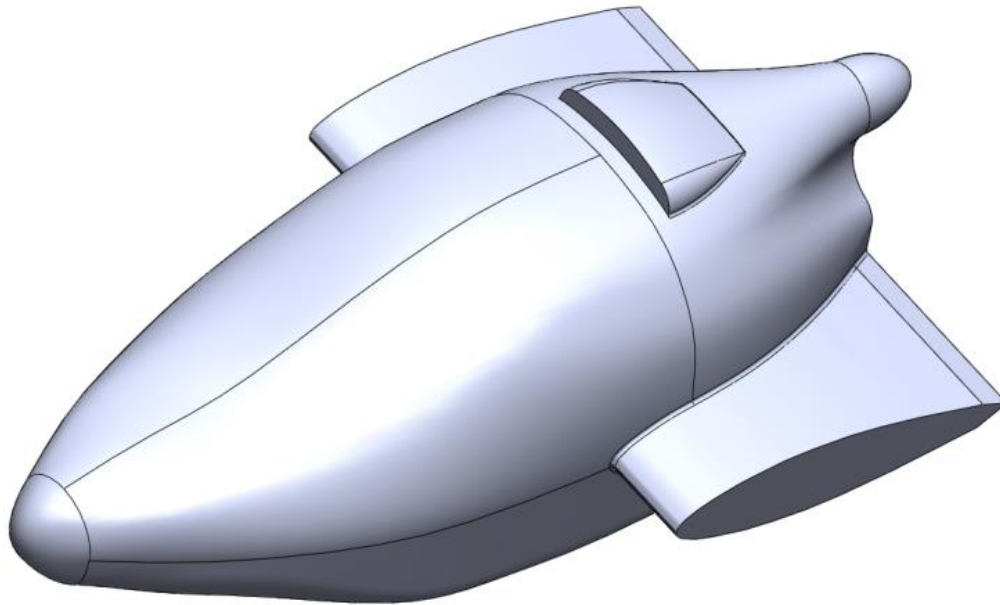


Figure 4-3: Upper Intake Scoop

Before analysis of the internal flow could begin, it was necessary to determine the flow conditions at the intake scoop's inlet. To do this, an external fuselage flow analysis without the intake scoop was performed at the rotation speed velocity of 82.3 ft/s using the method described in section 2.1. In results post-processing, the mid-plane velocity at the location of the intake scoop was sampled and found to be 78.3 ft/s. This was the velocity assigned to the inlet boundary condition for the internal flow analysis. Using the method in section 2.3, the internal flow mesh was generated with 1.48 million elements.

In the un-baffled configuration, the intake air followed the contour of the roof of the engine compartment, was directed downward by the spinner back-plate, and exited via the outlet with some internal flow recirculation. This was a clear indication that a baffle was necessary to direct the intake airflow over the engine's cylinders. To rectify this, a baffle was positioned at the root of the intake air scoop, and was angled down by 68° . With a length of 8.3" at the mid-plane, it extended just behind the engine's integrated gearbox as seen in Figure 4-4.

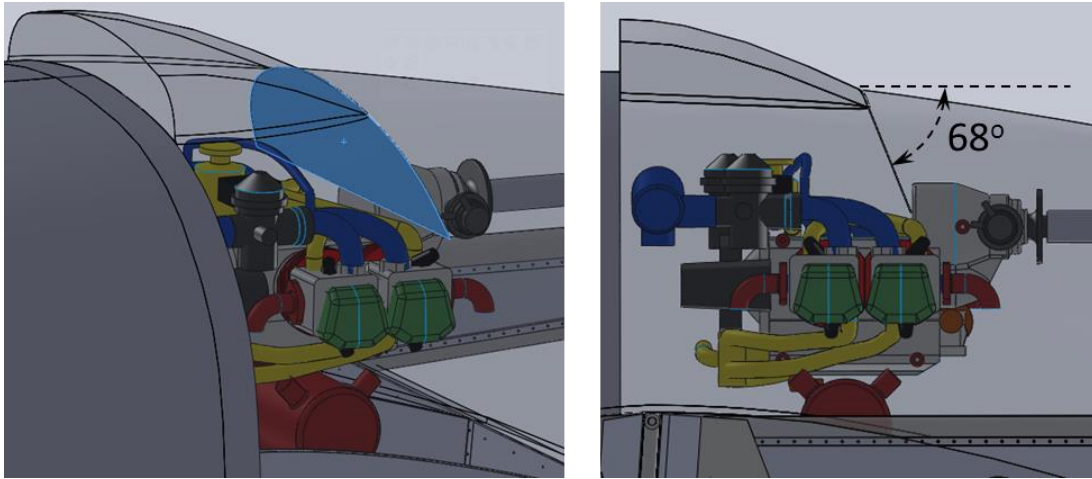


Figure 4-4: Upper Baffle Location

Internal flow analysis with the inclusion of the upper baffle showed that the flow was directed over the engine's cylinders. However, there was little to no flow over the exhaust components and the engine compartment outlet velocities were low. This indicated that most of the energy in the intake airflow was being dissipated inside the engine compartment – a phenomenon which increases the cooling drag of the aircraft. To induce low pressure in the lower portion of the engine bay, a small belly intake scoop was added with dimensions of 9" width, 2" height, and 9" length. Half-inch radius fillets blended the scoop to the fuselage. Another benefit to this lower scoop was that it would act as a vent for the 'chimney effect' when the hot engine cools down after shutdown. Furthermore, FOD ingestion was not so much a concern for this scoop due to its smaller size.

Using the external fuselage CFD analysis at rotation speed, the mid-plane velocity at the lower scoop inlet was sampled. It was found that the inlet velocity was 96.78 ft/s. After updating the internal flow model, the results showed that the airflow ran along the bottom of the fuselage and exited via the outlet after being diverted upwards by the aft spar. There was no observable effect on the airflow from the upper scoop. This prompted a re-configuration of the lower scoop; it was widened to span the 24.5" wing center bay and was shortened to a height of 1". The final configuration of the lower scoop is seen in Figure 4-5:



Figure 4-5: Lower Intake Scoop

Lower baffles were also positioned in the lower engine compartment for two purposes. Firstly, baffles extending the wing center section ribs to the floor of the engine compartment were placed as seen on the left in Figure 4-6. This served to reduce the fluid volume of the engine compartment to reduce random turbulent flow. Secondly, a baffle angled at 52° that spanned the center bay was positioned as seen on the right in Figure 4-6 to direct the airflow from the lower scoop up toward the exhaust. This baffle had a length of 15.2" which allowed it to extend to the same plane as the lower limit of the engine compartment's cooling outlet.

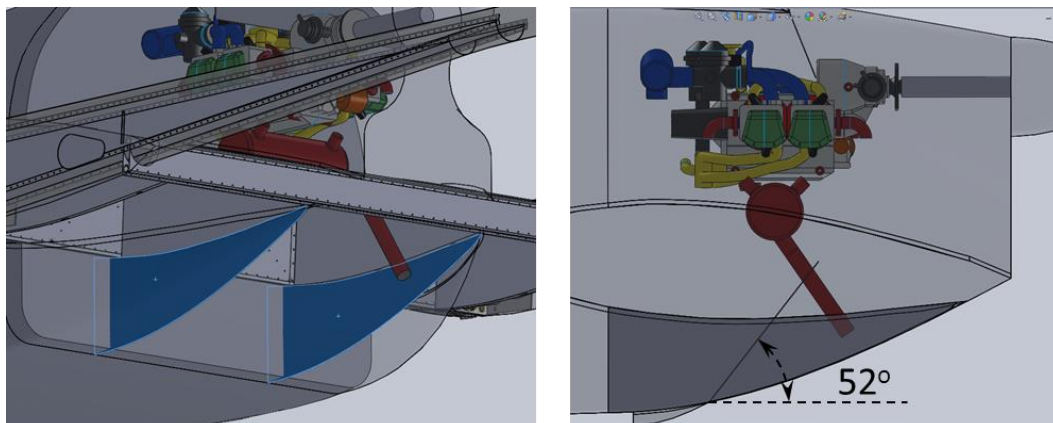


Figure 4-6: Lower Baffles

The final internal flow analysis yielded favorable results as seen in Figure 4-7. The lower baffles and re-designed lower inlet scoop effectively directed airflow upwards to the exhaust components. The flow from the lower scoop also merged with the flow from the upper scoop aft of the engine such that the net flow was directed through the outlet with less turbulence than seen in previous internal flow analysis. It is important to note that if the engine position is updated in the future with the Allegro engine suspension frame and exhaust system, the angles and position of the baffles will need to be revised so that the cooling airflow is adequately directed over critical cooling components.

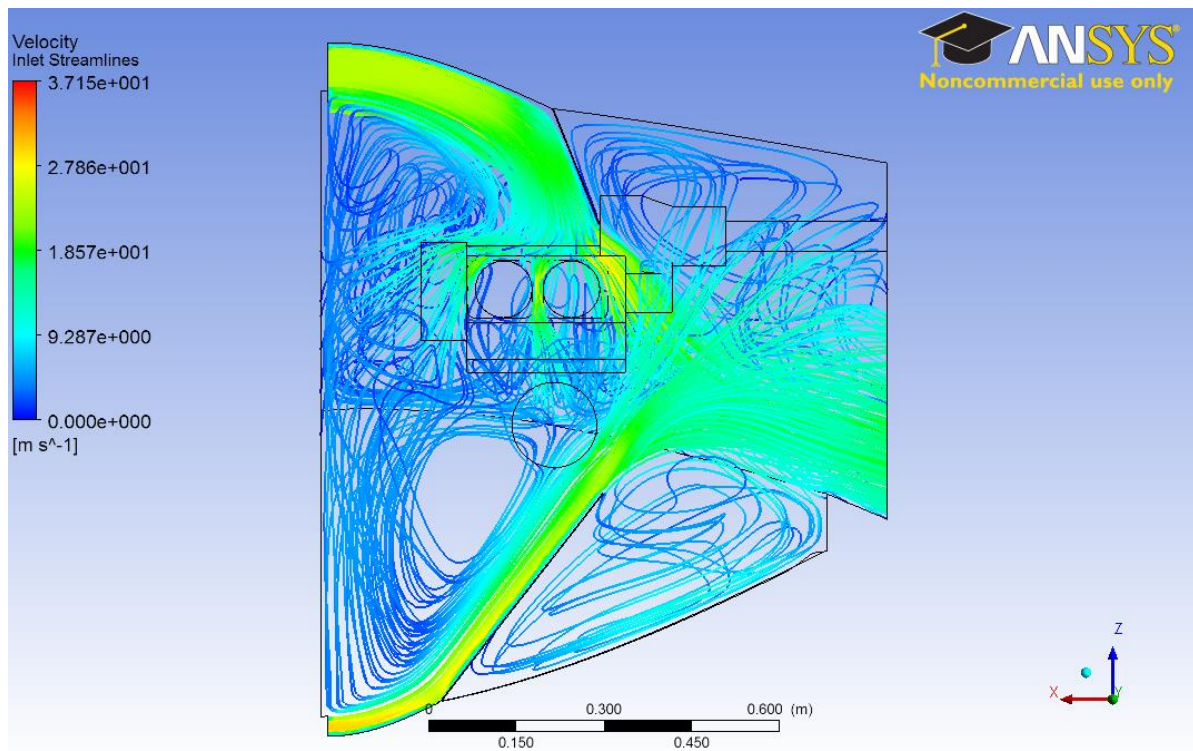


Figure 4-7: Internal Flow Results for Final Baffle and Inlet Scoop Configuration

The internal flow rendering of the intermediate design steps is provided in Appendix C. The geometry of the baffles and intake scoops is detailed in Appendix D.

5 Additional Considerations

As described in the scope of this project, the aft portion of the Vampire fuselage was re-designed to reduce drag and to house the Rotax 912 ULS engine. Analysis and design of components to direct cooling airflow over the engine's critical cooling components was also performed. Before this project could be concluded, it was also within the scope to provide estimates of weight savings considering the change in installed engine, airflow baffles, and planned modification of the fuselage composite layup. Since the engine position was revised, an investigation into propeller clearance was also performed. Lastly, it was shown that the new fuselage design could be manufactured from the existing prototype fuselage molds by means of installing plugs.

5.1 Full Assembly

The new fuselage configuration was integrated to Sadler Aircraft's full aircraft CAD assembly as seen in Figure 5-1. A dimensioned 3-view drawing of the new Vampire is available in Appendix E.

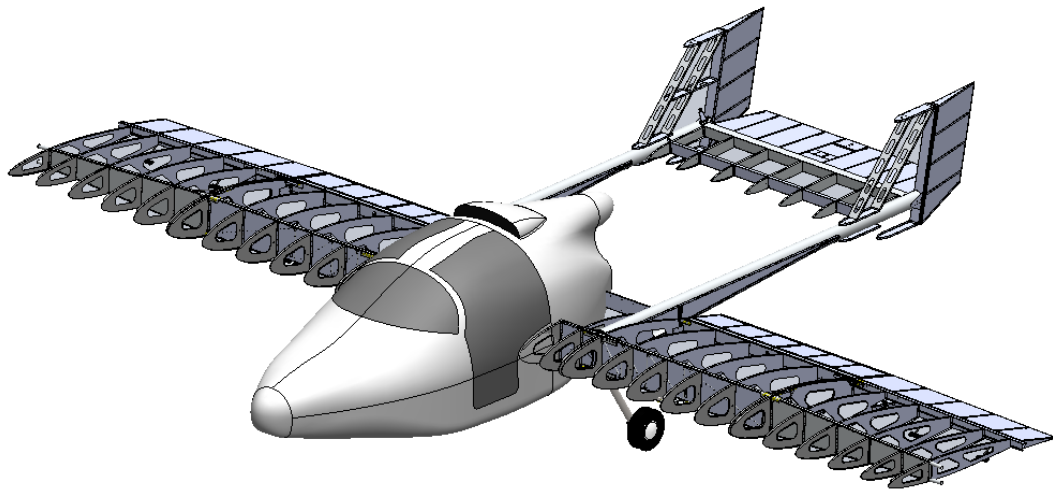


Figure 5-1: New Fuselage Integrated with the Wing and Tail Components

The new fuselage was designed to be a direct drop-in replacement from the prototype fuselage where the wing structure is positioned and fastened to the fuselage firewall in the same location and manner. This reduces the necessary spatial integration and structural analysis required for future work on the Vampire.

5.1.1 Propeller Clearance

Integration of a new engine often requires a re-analysis of the aircraft's performance so that a propeller may be chosen to give the aircraft its desired performance or to limit it so it remains in the bounds set by the LSA category. It was beyond the scope of this project to perform this analysis, but the full aircraft assembly could be used to determine how much clearance is available for propeller selection given the new engine positioning.

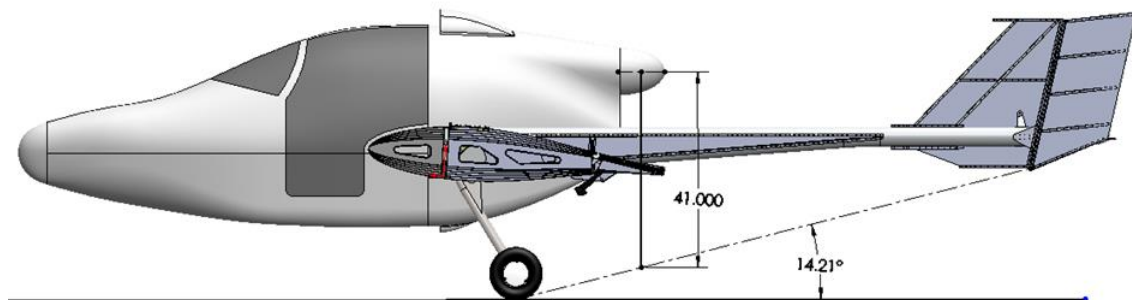


Figure 5-2: Propeller Clearance

According to Figure 5-2, a line drawn from the wheel contact point on the ground to the lowest point on the empennage gives a maximum tip-back angle of 14.2°. A radius drawn from the center of the spinner to this line shows that there is about 41" of clearance for a propeller. This is more clearance than the prototype Vampire since the Rotax 912 ULS is located higher and further forward than the Jabiru 3300. It is important to note that wheel deflation and landing gear deflection due to weight and landing loads were not accounted for in this measurement. Thus, a factor of safety in the stated clearance measurement should be used when selecting a propeller.

5.2 Estimated Weight Impacts

One of the prototype Vampire's problems was its MTOW as a result of a heavy fuselage composite layup schedule. Though not directly addressed in this project, an estimate of the potential weight savings could be made using the CAD models. This included the weight change caused by the cooling baffles, engine swap, and alteration of the composite layup schedule for the fuselage. In its current state, the prototype fuselage is fabricated using a chopped fiberglass layup common to boat manufacturing. These layups are typically much heavier than aircraft composites which often consist of layers of fiberglass sandwiching a foam or honeycomb core. It was reasonable to assume that once a detailed structural analysis for the new Vampire fuselage is performed, the resulting layup schedule would be similar to that of LSA America's Allegro light sport aircraft. The company provided a composite panel from the Allegro's fuselage and its composition is shown in the following figure:

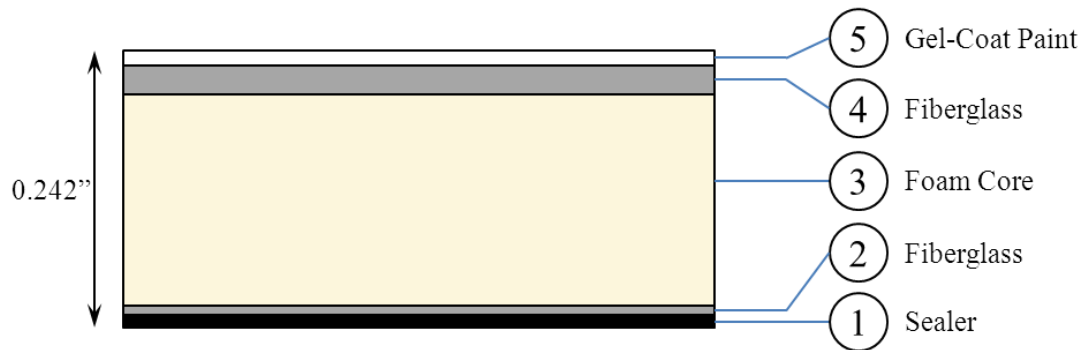


Figure 5-3: Allegro Composite Sandwich

The composite layup consisted of five components totaling 0.242" in thickness: A foam core was sandwiched between two layers of fiberglass with the outer fiberglass layer being thicker than the inner layer. The outer-most layer was coated with gel-coat paint while the inner layer was coated with a moisture sealant. A sample of dimension 4.07"x2.61"x0.242" was cut from the supplied panel so that its density could be calculated. The sample had a mass of 8.05×10^{-4} slug, giving it a density of 0.541 slug/ft^3 (279 kg/m^3). For comparison, a sample

fiberglass layup was fabricated and measured to estimate the density of the prototype vampire's fuselage composition. The sample's dimensions were 4.08"x2.65"x0.169" and it had a mass of 3.41e-3 slug. This resulted in a density of 3.22 slug/ft³ (1661 kg/m³). Both the new and prototype fuselages were assumed to have wall thicknesses equal to that of the 0.242" thick Allegro panel sample that was provided. For simplicity, any firewalls, bulkheads, and other internal structures were omitted from this estimate. The resulting weight estimates were 246 lbs and 39.8 lbs for the prototype and new fuselage shells respectively.

Absent from the prototype fuselage were baffles in the engine compartment. In the case of the new fuselage configuration, four baffles were required to properly direct cooling airflow over critical components. So as to not deflect or bend when redirecting high intake flow velocities, they needed to be fabricated from stiff but lightweight material. It was decided that the baffles were to be fabricated from 1/16" aluminum alloy sheeting and cut either by Computer Numeric Control (CNC) machining or by hand. Using the default SolidWorks density for 1060 alloy aluminum, the upper baffle weighed 1.04 lbs, the center-section rib extension baffles weighed 1.29 lbs each, and the lower angled baffle weighed 2.63 lbs. The combined weight of the baffles in the new fuselage was 6.25 lbs.

The last component considered for weight impacts was the installed weight of the Rotax 912 ULS engine. The prototype fuselage was designed to accommodate a Jabiru 3300 six-cylinder boxer engine with an installed weight of 178 lbs [13]. The Rotax engine, on the other hand, had an installed weight of 140.6 lbs [14]. This shaved 37.4 lbs off the new configuration. Taking the difference of the total weight impacts from the two fuselages, a theoretical weight reduction of about 237 lbs can be realized. Table 5-1 summarizes the weight impacts from the aforementioned components.

Table 5-1: Weight Impact Summary

Component	Prototype Fuselage (lbs)	New Fuselage (lbs)
Fuselage Shell	246.0	39.79
Baffles	--	6.25
Engine	178	140.6
Total:	424.0	186.6
Δ	-237.4	

The engine specifications, weight impact, and drag reduction were also used to estimate performance impacts. The power required for straight and level flight in standard sea level atmospheric conditions at 120 kts was calculated using Equation 3-1. The drag coefficient for the whole aircraft was assumed to be twice the drag coefficient of the fuselage and semi-wing section used in the fuselage drag analysis. For the baseline fuselage, the estimated C_D was 0.030. For the new fuselage, the drag coefficient was $C_D = 0.0264$. Power available was assumed to be the maximum continuous power rating for the engines: 107hp and 95hp for the Jabiru [13] and Rotax [14] respectively. After accounting for an assumed propeller efficiency of 70%, the power available was reduced to 74.9hp and 66.5hp respectively.

The power required for the baseline aircraft at 1320 lbs was 72.1hp which left enough excess power to attain an estimated maximum cruise speed of 121.5 kts. For the new fuselage configuration assuming a weight loss of 237 lbs and power required of 63.5hp from the drag reduction, the resulting estimated maximum speed was 121.9 kts. The performance summary is tabulated in Table 5-2 below.

Table 5-2: Performance Estimate Summary

Parameter	Baseline Aircraft	New Configuration
C_D	0.030	0.028
Engine Power (hp)	107	95
Power Available (hp)	74.9	66.5
Power Required (hp)	73.1	63.5
Weight (lbs)	1320	1083
Estimated V_{max} (kts)	121.5	121.9

5.3 Mold Plug

LSA America planned to manufacture Vampire fuselages by performing composite lay-ups in the molds purchased from Sadler Aircraft. Since the new fuselage design is identical to the prototype forward of the firewall and the aft section is smaller in overall dimension, it is possible to modify the existing molds with plugs so that the new fuselage can be made from these same molds. Figure 5-4 shows the prototype fuselage overlaid on the new fuselage, and Figure 5-5 shows the plug geometry after volume subtracting the two fuselages.

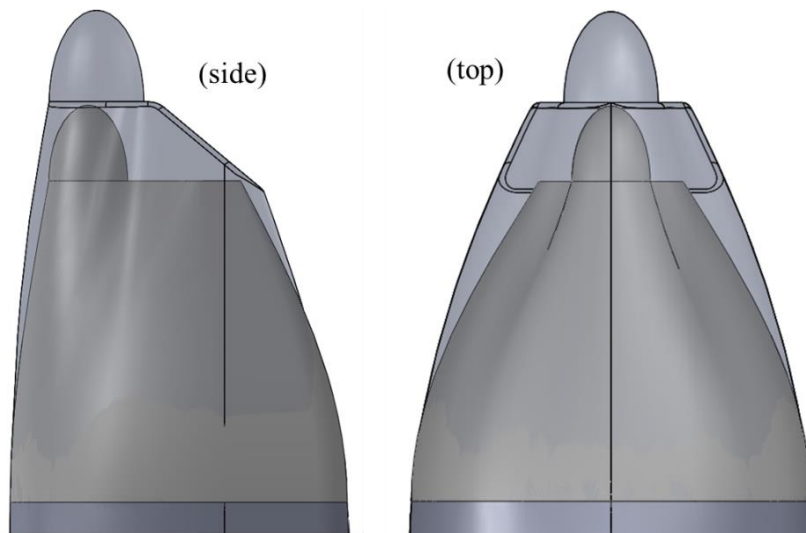


Figure 5-4: New and Prototype Fuselage Aft Section Comparison



Figure 5-5: CAD Model for Mold Plug

Details such as dimensions and the location of the parting plane of the existing mold were not provided, so it was not possible to define the parting plane line for the upper and lower half split of the plug. However, creating separate CAD models for the upper and lower plugs is a simple process once the parting plane is known. It is intended for the plug to be fabricated by routing excess material from a block of foam or medium to high density fiberboard. Once fabricated and finished, the plug can then be bonded to the existing molds. For reference, Table 5-2 contains dimensional and volume information to assist in sourcing material with which to fabricate, finish, and bond the plug.

Table 5-3: Mold Plug Statistics

Parameter	Value
Max. Length (in)	45.5
Max. Width (in)	47.4
Max. Height (in)	37.8
Volume (in ³)	10,202
Outside Surface Area (in ²)	4,344
Inside Surface Area (in ²)	3,629

6 Conclusion

At the request of LSA America, a new fuselage configuration for the Vampire Light Sport Aircraft was designed. The primary goals were to reduce the base drag of the existing prototype's fuselage and to integrate the Rotax 912 ULS engine. To accomplish these goals within the scope and timeline for this project, an analysis method using the ANSYS 13 Workbench Fluent suite was developed to evaluate the aerodynamic performance of fuselage configurations and to visualize cooling airflow within the engine compartment. After an iterative design process, a drop-in replacement fuselage was designed that reduces drag by 11.5% resulting in a reduction of power required at a velocity of 120kts by 4.4hp. The new design was accomplished by modifying only the fuselage section aft of the firewall; this facilitates production of the new fuselage by only requiring the addition of plugs to the existing molds.

Provisions were also made to integrate the Rotax 912 ULS engine to the new Vampire fuselage. Since information on the desired engine suspension frame and exhaust system were unavailable, integration work was performed assuming that the stock frame and exhaust system as described in its installation manual would be used. The engine was positioned in the engine bay, and ram air intake scoops and airflow baffles were designed such that cooling airflow reached critical engine components. In this configuration, an output extension shaft of 10.9" was still required. It was beyond the scope of this project to perform detailed integration work, so the location of components such as the engine oil container, radiators, connecting hoses, and baffle fasteners were not defined. It is expected that future integration work will incorporate the Allegro LSA's engine mount and exhaust system as originally requested by LSA America; this will require revision of the location, geometry, and orientation of the airflow baffles. However, the method and groundwork performed in this project will expedite and facilitate that process.

6.1 Future Work

A possible avenue of future research would be to further develop the CFD application methods presented in this document. If unbounded by the limits of the ANSYS student license, there is potential for the external fuselage meshing and analysis method in Fluent to yield results that better align with experimental data. Furthermore, it may be of interest to expand this method such that external fuselage aerodynamics and internal flow are modeled in the same simulation; this would expand the results envelope to include more accurate intake flow conditions, cooling drag, and overall fuselage drag that accounts for ram-air intake and outlet flow.

The design work presented in this paper represents only a fraction of what can be done to make the Vampire Light Sport Aircraft a successful and profitable product. Structural analysis, composite layup schedule design, performance and handling analysis, and detailed-design and integration work are still required before the new fuselage configuration presented in this document can be implemented. The next step would be to structurally analyze the new fuselage and develop a new composite layup schedule. Using the Allegro's composite structure as a benchmark, significant weight savings of 200 lbs or more can be realized if the chopped fiberglass layup is replaced with a foam-core composite sandwich. Further analysis would also be required to ensure that attachment of the wing and engine suspension frame to the firewall meets ANSI structural requirements for the LSA category. Replacement of the Jabiru 3300 with the Rotax 912 ULS engine necessitates a performance and handling re-evaluation. The change in aerodynamics and mass of the new fuselage and its components has an effect on the dynamic modes of the aircraft, and they should be analyzed to ensure safe and satisfactory aircraft handling. Furthermore, work can be done to select a new propeller since the reduction in drag of the new fuselage may have expanded the Vampire's performance capability beyond the LSA category limits.

6.2 Concluding Remarks

Being a part of the Vampire re-design project has allowed me to further develop my aircraft design skills and multi-disciplinary perspective. Many aspects of performing design work on aircraft in the Light Sport category require that the engineer be mindful of multiple, and often conflicting, design goals that must be balanced to arrive at a successful design. This project also challenged my time management skills and ability to quickly learn to use new tools to develop methods to get the job done.

The methods presented in this thesis for the aerodynamic drag analysis of fuselages and cooling airflow are not limited to LSA applications. If appropriately scaled, relatively fast evaluations of Unmanned Aerial Vehicles, general aviation aircraft, rockets, etc. can be performed by engineers who do not need to be experienced in CFD. It is my hope that the work presented in this document will be used by current and future engineers who are facing these sorts of design challenges.

References

- [1] U.S. Department of Transportation, “FAA Order 8130.2G”, *Federal Aviation Administration*, 31 August, 2010. pp 4-15.
- [2] Pew, G., “LSA Company for Sale, Sadler Vampire”, *AVFlash News*, <http://www.avweb.com/avwebflash/news/sadler_vampire_company_lsa_for_sale_light_sport_aircraft_202628-1.html>, 26 May, 2010. Accessed 6 March, 2013.
- [3] Green, B. E., “Computational Prediction of Nose-Down Control for the Pre-Production F/A-18E at High Angles of Attack”, *AIAA Atmospheric Flight Mechanics Conference and Exhibit*, AIAA 2007-6724. pp 4-5.
- [4] SAS IP, Inc., “ANSYS Fluent Tutorial Guide”, *ANSYS Inc.* Release 14.0, November 2011.
- [5] Jacobs, E. N., “Sphere Drag Tests in the Variable Density Tunnel”, NACA TN-312, August 1929.
- [6] Raymer, D. P., “Special Considerations in Configuration Layout”, *Aircraft Design: A Conceptual Approach*, 2nd ed, American Institute of Aeronautics and Astronautics, Washington D.C, 1992, pp. 155-156.
- [7] Hoerner, S. F., “Pressure Drag”, *Fluid-Dynamic Drag*, 1965, pp. 3-22.
- [8] Hoerner, S. F., “Pressure Drag”, *Fluid-Dynamic Drag*, 1965, pp. 3-18.
- [9] Raymer, D. P., “Propulsion and Fuel System Integration”, *Aircraft Design: A Conceptual Approach*, 2nd ed, American Institute of Aeronautics and Astronautics, Washington D.C, 1992, pp. 225-226.
- [10] BRP Powertrain GmbH@Co. KG., “Installation Manual for Rotax Engine Type 912 Series”, 2nd Ed, Rev 0. 2012.
- [11] Windcraft Oy, “A 3D CAD Model of Rotax 912 Engine”, <<http://www.windcraft.fi/download/3dmodels.htm>>, 2013. Accessed 29 January, 2013.
- [12] Raymer, D. P., “Thrust-to-Weight Ratio and Wing Loading”, *Aircraft Design: A Conceptual Approach*, 2nd ed, American Institute of Aeronautics and Astronautics, Washington D.C, 1992, pp. 87.

- [13] Jabiru Pacific LLC, “Jabiru 3300 120hp engine features”, *Jabiru Aircraft & Engines – Light Sport Aircraft*, <<http://www.jabirupacific.com/specs/3300.htm>>, 2008. Accessed March 16, 2013.
- [14] Aero Propulsion Technologies, “Rotax 912 ULS CDCI 100HP”, *Engines*, <http://www.rotaxservice.com/rotax_engines/rotax_912ULSs.htm>, Accessed March 14, 2013.
- [15] Anderson, J.D, “Elements of Airplane Performance”, *Introduction to Flight*, 6th Ed, McGraw-Hill, New York, New York, 2008, pp. 430.

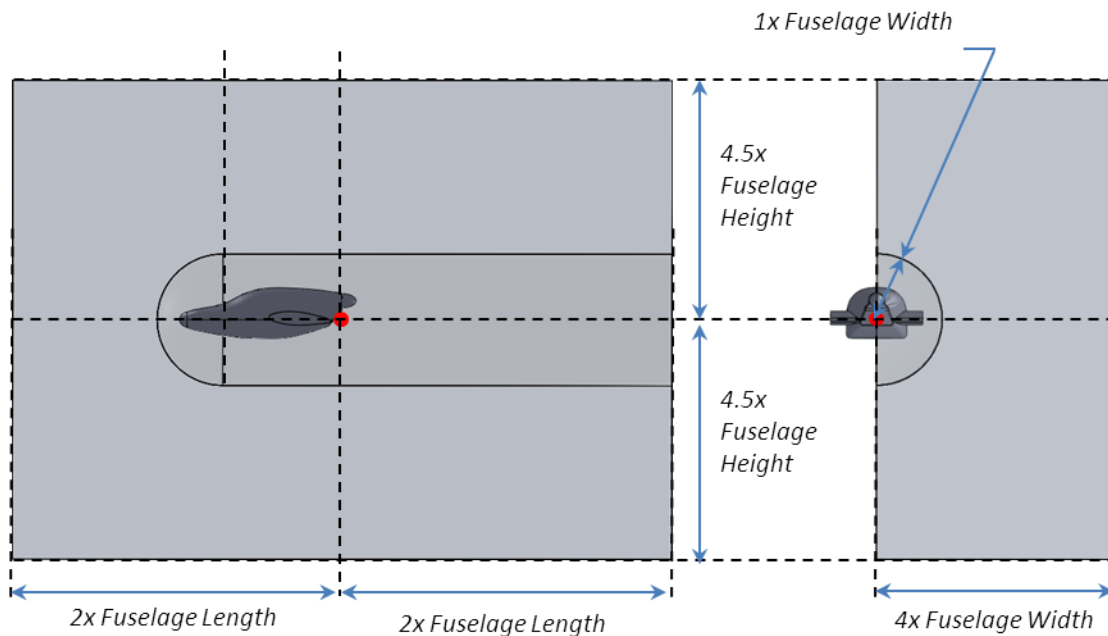
Appendix

Appendix A – Method User Guide

This guide is intended for users to follow as step-by-step instructions, and is valid for ANSYS Workbench 13 and 14. The resulting mesh and analysis provides for coarse far-field results with a finer mesh and higher resolution near the fuselage or part and in the wake behind it.

CAD Modeling

- 1) Model your fuselage or part as a solid.
- 2) Model the 2-volume computational domain as two separate solid parts. They should be coincident when placed in the assembly. Use the figure below as a size guide for the computational domain.



Setting Up the Project

- 1) Launch ANSYS Workbench
- 2) Select '**Fluid Flow (FLUENT)**' and drag it to the project schematic window
- 3) Name and save the project.

Importing SolidWorks Geometry

- 1) In the Project Schematic, Right Click 'Geometry' → 'Edit Geometry...'
- 2) In the Design Modeler interface, 'File' → 'Import External Geometry File...', and select your SolidWorks assembly.
- 3) In the tree outline, **Right Click** the 'Import1' label → 'Generate'
- 4) Once the geometry has generated, click 'Create' → 'Boolean'
 - Set 'Operation' to 'Subtract'
 - Select your domain or wake-core as the 'Target Body'
 - Select the fuselage or part as the 'Tool Body'
 - Set 'Preserve Tool Bodies' to 'No'
 - **Right Click** the 'Boolean1' label → 'Generate'
- 5) Expand the 'Parts and Bodies' label in the tree outline
 - Select each body and set 'Fluid/Solid' to 'Fluid' in the 'Details of Body' options menu.
- 6) Close Design Modeler. The model will automatically update to the Workbench project.

Meshing

- 1) In the Project Schematic, Right Click 'Mesh' → 'Edit...'
- 2) When opening the Mesher for the first time, you will be prompted to select general meshing options. Use the default tetrahedral meshing options and click 'Apply'.
- 3) In this step, you will create your named selections. Start by enabling face selection by clicking on the  icon in the upper toolbar. To select multiple faces, hold **Ctrl** and **Left Click** on the faces you wish to select.
 - Select the inlet face(s). **Right Click** → 'Create Named Selection' → Name the face(s) 'inlet'
 - Repeat the process for 'outlet'
 - Repeat the process for 'symmetry'. *Note that you will use the symmetry boundary condition if your part is left-right half symmetric. This requires that only half the computational domain be modeled. If your part is not symmetric, skip this step.*
 - Repeat the process for any selection of faces you wish to monitor lift, drag, or moments on. Name them anything other than the indicated keywords.
 - If meshing with two or more volumes, create 'interface' named selections. In the two-volume example given, both the coincident faces on the domain AND on the wake-core need to be given an 'interface' name.

It is important to note that keywords such as 'inlet', 'outlet', 'symmetry' and 'interface' are automatically detected by Fluent. Naming them as such reduces your workload in the Fluent Set-Up steps.

- 4) In this step, you will create element size controls for the different named selections. Make sure that the **Mesh** label is selected in the **Outline** menu on the left side of the screen.

With the  face selection option enabled, hold **Ctrl** and **Left Click** to select multiple faces.

- Once the appropriate faces are selected, **Right Click** → **Insert** → **Sizing**
- Under **Element Size**, specify the element size using the sizing chart below.

Surface	Far-Field & Inlet	Outlet	Interfaces	Aircraft/Part
% Ref. Chord	22	9.5	4.4	0.95

- 5) Now it is time to set up the general and automatic mesh options. Select **Mesh** in the outline window. Expand the **Sizing** label.
- Set **Used Advanced Sizing** to **Off**
 - Set **Relevance Center** to **Fine**
 - Set **Smoothing** to **High**
 - Set **Transition** to **Slow**
- 6) Expand the **Inflation** label.
- Set **Inflation Option** to **Last Aspect Ratio**
 - Set **First Layer Height** to the size of your smallest defined element from Step 4
 - Set **Maximum Layers** to 1000
- 7) In the upper toolbar, click **Mesh** → **Generate Mesh**
- 8) Inspect the mesh to make sure it is under 1.5 million elements in the **Statistics** tab. If it is satisfactory, click **Update**. Once this is finished, close the Mesher tool.

Fluent Set-Up

- 1) In the Workbench project schematic, **Right Click** **Setup** → **Edit...**
- 2) When the launch menu appears, leave all settings as default and click **OK**
- 3) Once Fluent Launches, Click on the **General** label in the **Problem Setup** tree.
 - Click **Units...**, and set-up the unit system you are using. Click **Close** when done.
- 4) Click on the **Models** label in the **Problem Setup** tree.
 - Select the aerodynamics model (third option down), Click **Edit...**
 - Select **Spalart-Allmaras**, and leave the settings at their default values.
 - Click **OK**
- 5) Click on the **Materials** label in the **Problem Setup** tree
 - Select **Air**

- 6) Click on '**Boundary Conditions**' in the '**Problem Setup**' tree
 - Set appropriate pressure and velocity conditions for the 'inlet'
 - Check that appropriate boundary conditions for the other named selections have been assigned.
- 7) Click on '**Mesh Interfaces**' in the '**Problem Setup**' tree
 - Click '**Create/Edit**'
 - Name the interface in the 'Mesh Interface' field
 - Select the two interfaces, and click '**Create**'
- 8) Edit the values in the '**Reference Values**' label in the '**Problem Setup**' tree
- 9) Click on the '**Solution Methods**' label in the '**Problem Setup**' tree
 - Change the option under 'Gradient' to 'Green-Gauss Node Based'
- 10) Click on the '**Monitors**' label in the '**Problem Setup**' tree
 - Select 'Residuals' and Click '**Edit...**'. Set your desired convergence criterion and reporting intervals. Click '**Ok**' when done.
 - Set up any lift, drag, and moment monitors in the same manner.
- 11) Click on the '**General**' label in the '**Problem Setup**' tree
 - Click '**Check**'. This checks the mesh and interfaces. If no errors occur, proceed with the next steps.
- 12) Click on the '**Solution Initialization**' label in the '**Problem Setup**' tree.
 - Select '**Hybrid Initialization**' and click '**Initialize**'. If the Hybrid initialization fails, proceed to the next sub-step. If it is successful, skip to step 12.
 - Select '**Standard Initialization**'. Input the inlet flow conditions in the fields and click '**Initialize**'.
- 13) Click on the '**Run Calculation**' label in the '**Problem Setup**' tree.
 - Click '**Check Case...**' and examine the report for any major errors or steps missed. If there are none, proceed to the next steps.
 - Input desired number of iterations in the 'Number of Iterations' field.
 - Click '**Calculate**'

Now your Fluent simulation should be running. Observe and residuals and lift/drag/moment monitors if any to make sure the simulation is converging in an expected direction. Once the simulation is done, it is ready for post-processing and results rendering.

Appendix B – Intermediate CFD Results

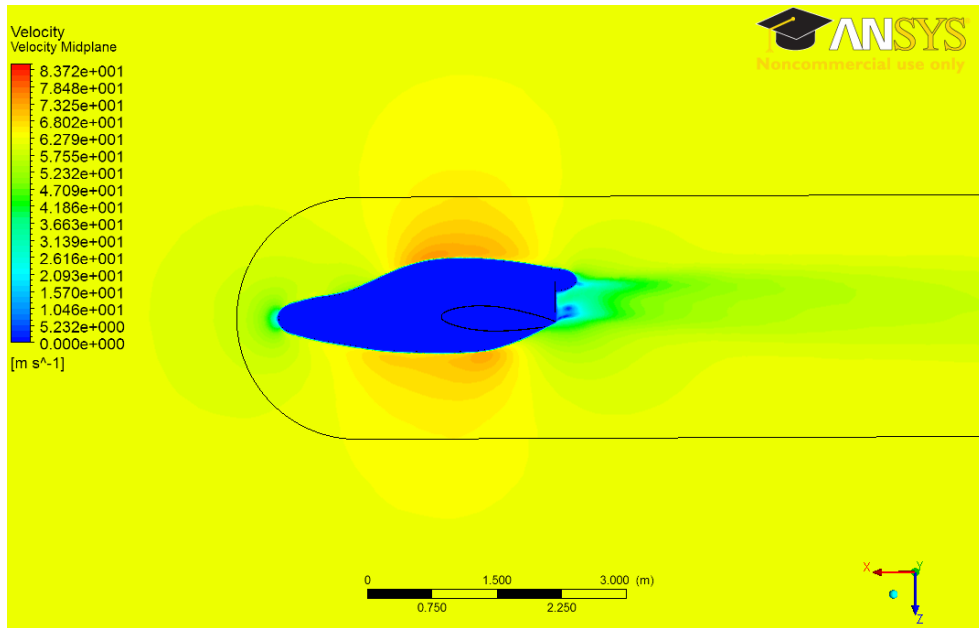


Figure 0-1: New Fuselage v1 Velocity Results

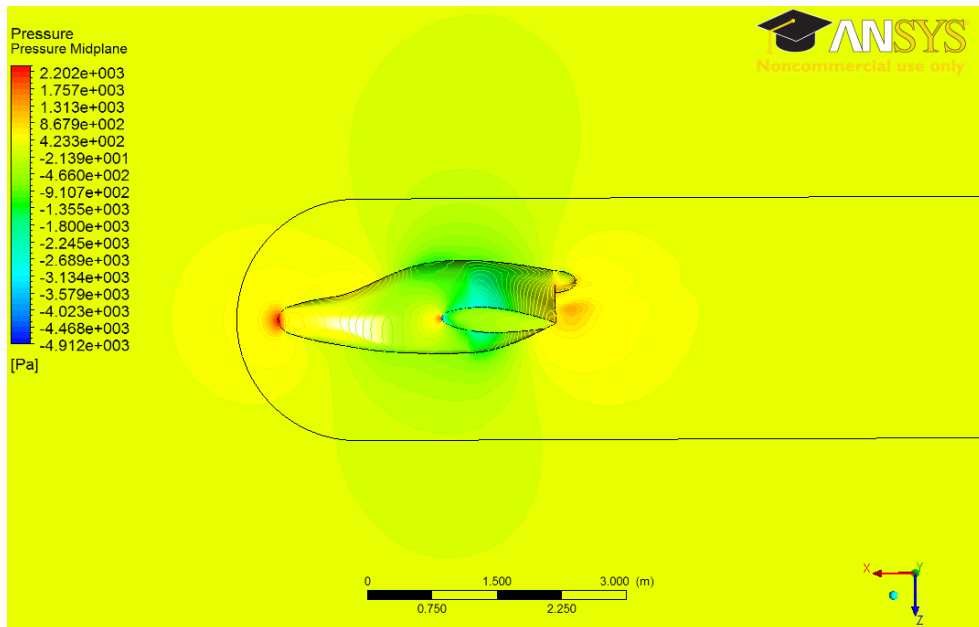


Figure 0-2: New Fuselage v1 Pressure Results

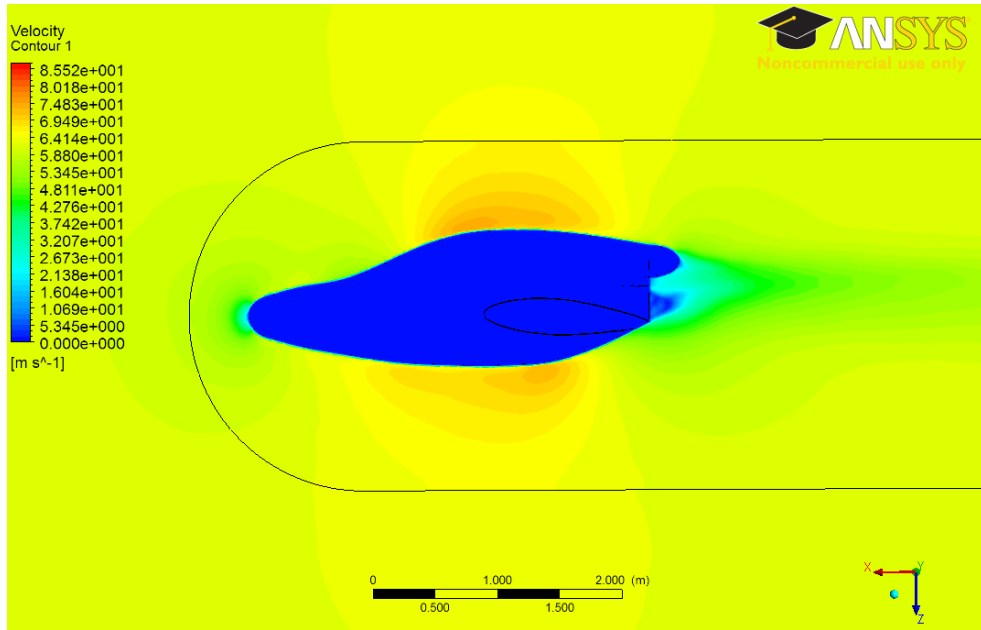


Figure 0-3: New Fuselage v2 Velocity Results

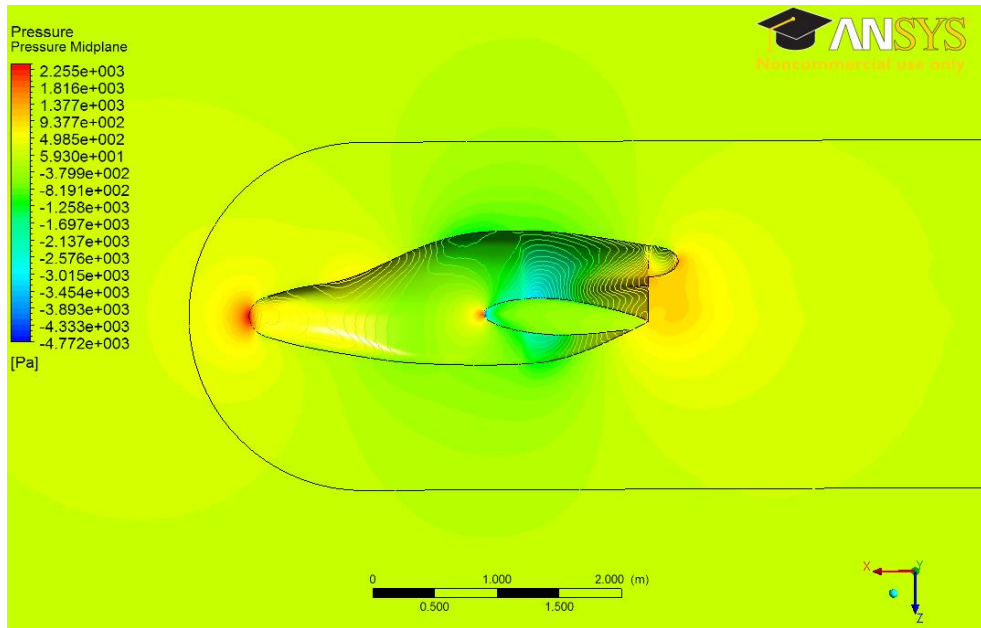


Figure 0-4: New Fuselage v2 Pressure Results

Appendix C – Intermediate Internal Flow CFD Results

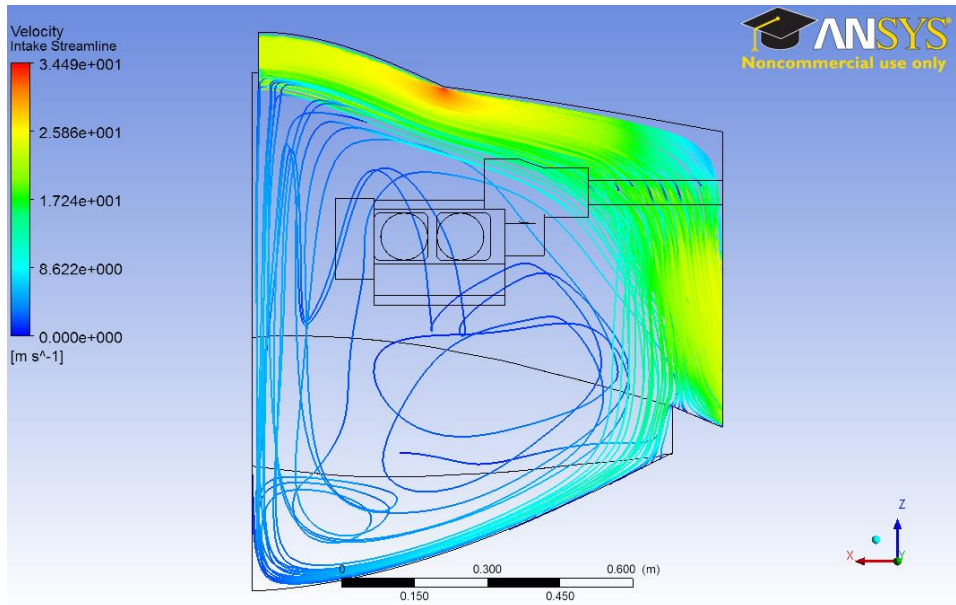


Figure 0-5: Un-Baffled Internal Flow

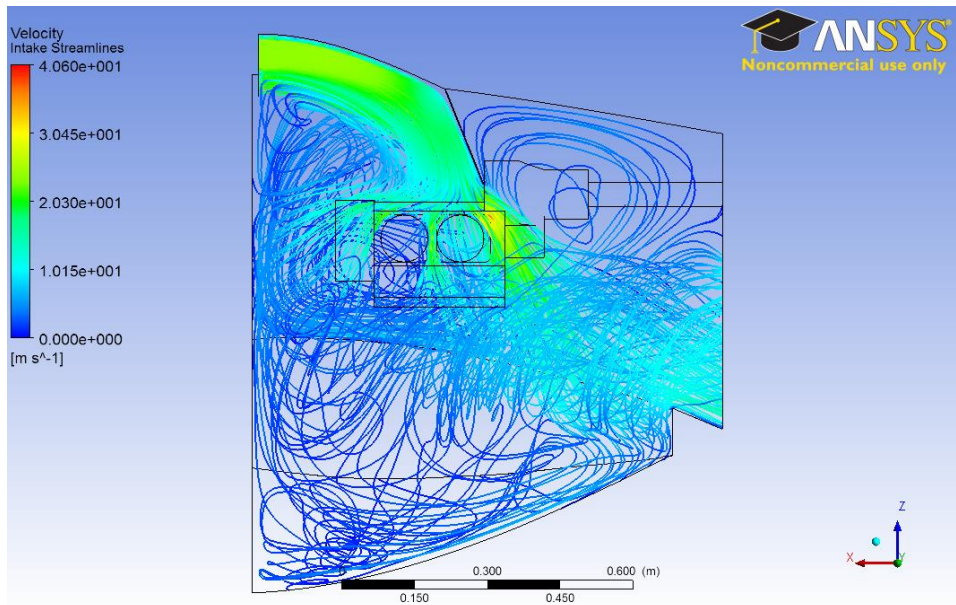


Figure 0-6: Internal Flow with Single Upper Baffle

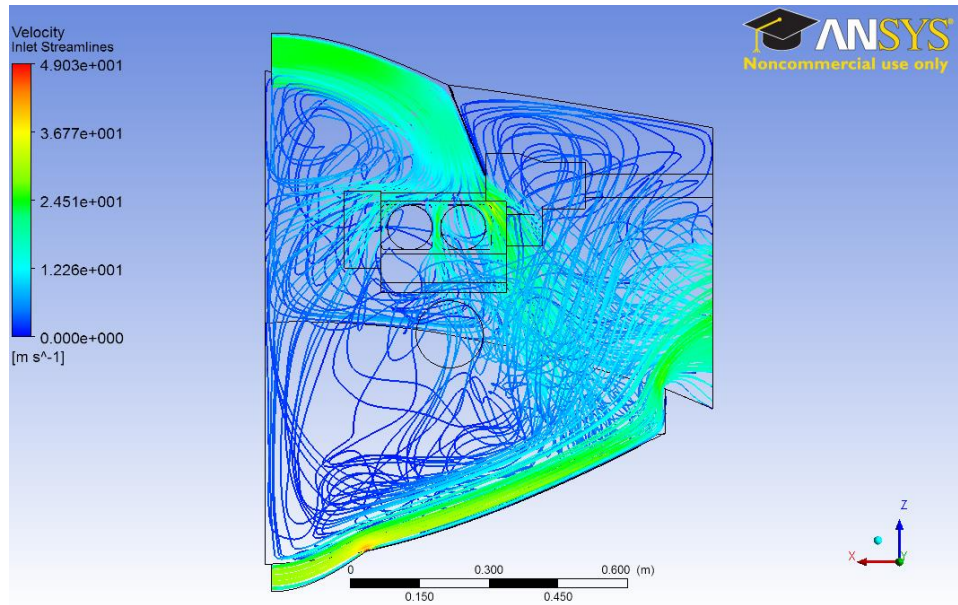


Figure 0-7: Internal Flow with Upper Baffle and Small Lower Inlet

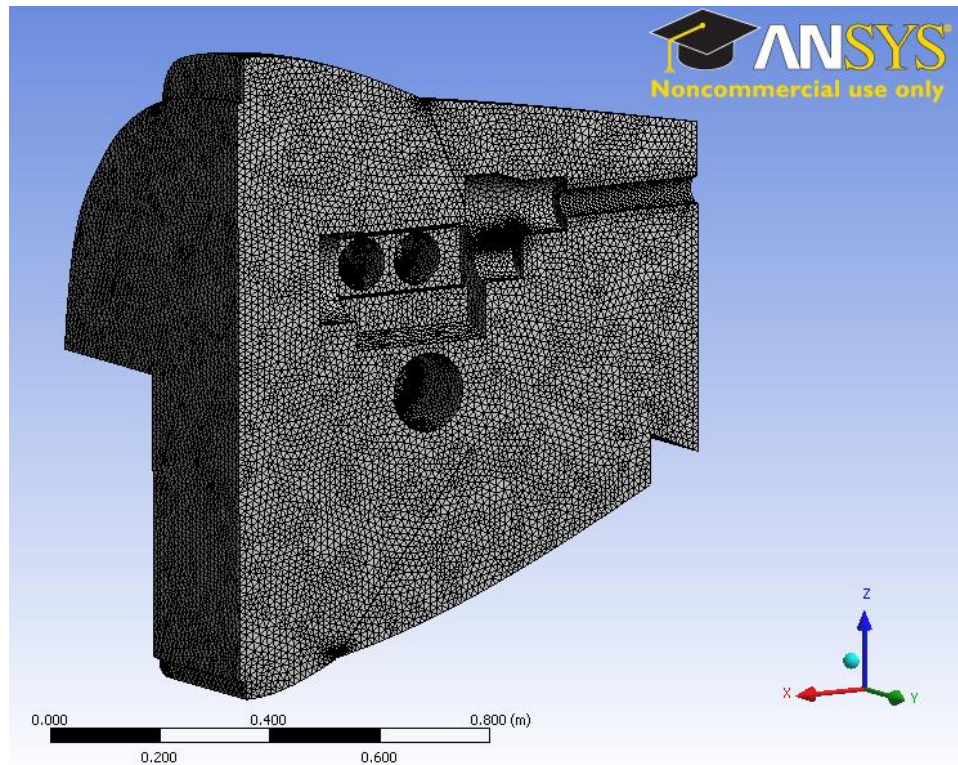


Figure 0-8: Mesh for Final Internal Flow Simulation

Appendix D – Cooling Component Geometry

UPPER INTAKE SCOOP

Units in inches unless otherwise specified.

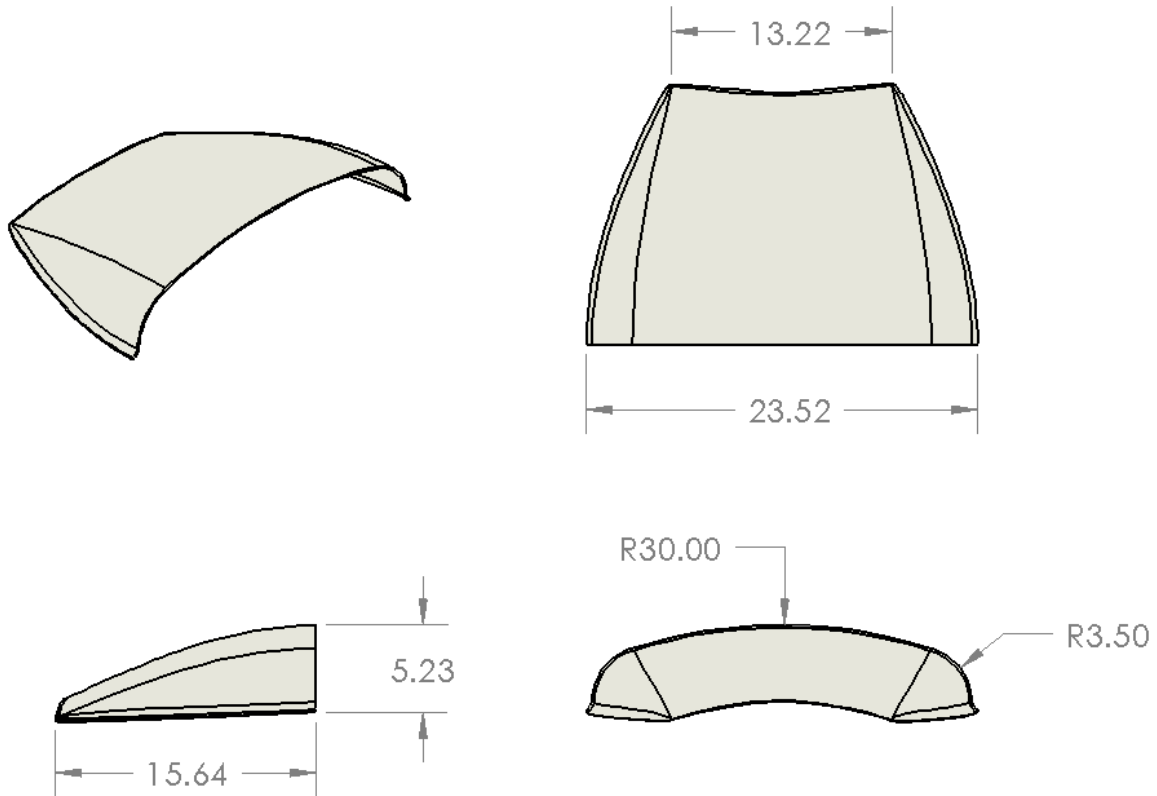


Table 0-1: Upper Intake Scoop Statistics

Parameter	Value
Outer Surface Area (in ²)	372.8
Inner Surface Area (in ²)	370.5
Fillet Radius (in)	0.5

LOWER INTAKE SCOOP

Units in inches unless otherwise specified.

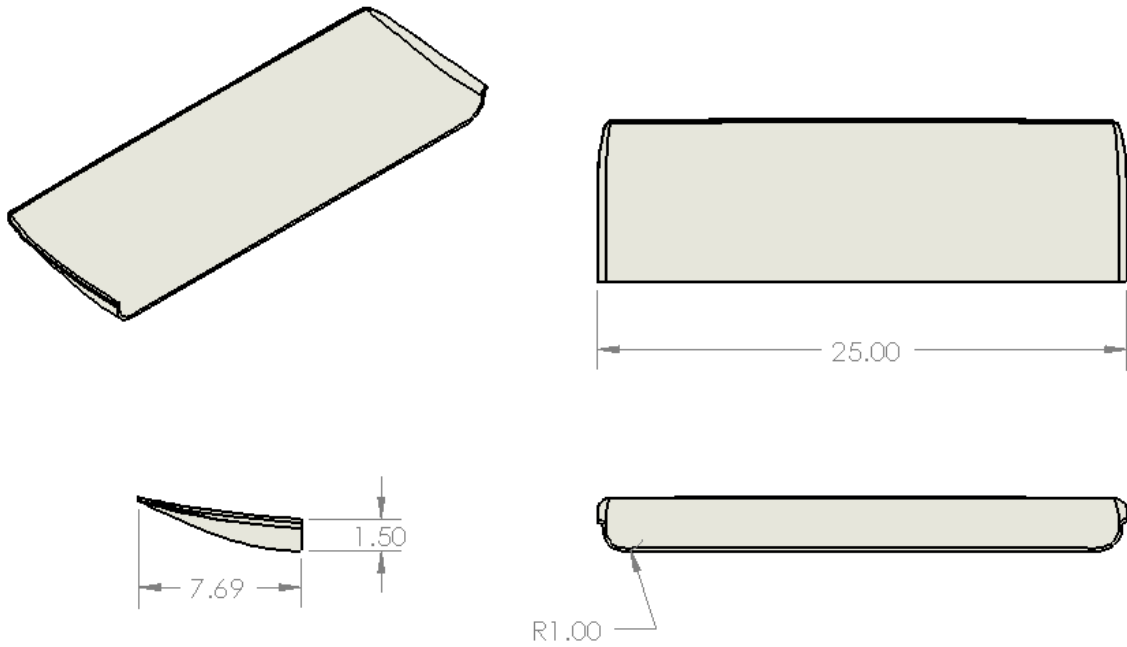
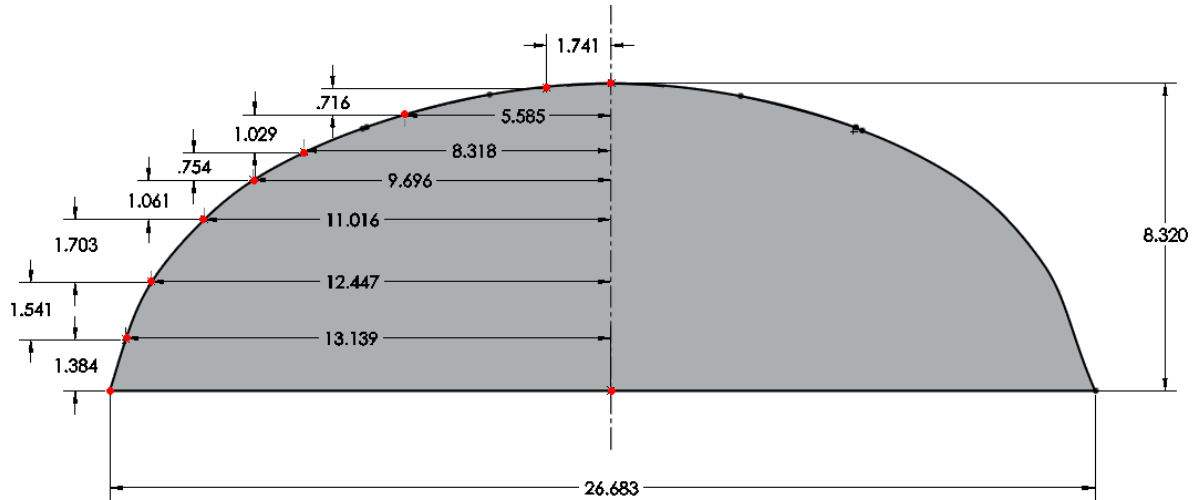


Table 0-2: Lower Intake Scoop Statistics

Parameter	Value
Outer Surface Area (in ²)	214.8
Inner Surface Area (in ²)	207.9
Fillet Radius (in)	0.5

UPPER BAFFLE

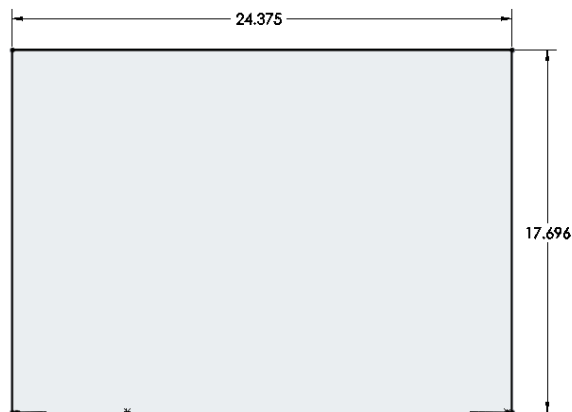
Units in inches unless otherwise specified. Dimensioned points are provided so a spline fit may be re-created to generate the baffle dimensions.



Area: 170.6in²

LOWER BAFFLE

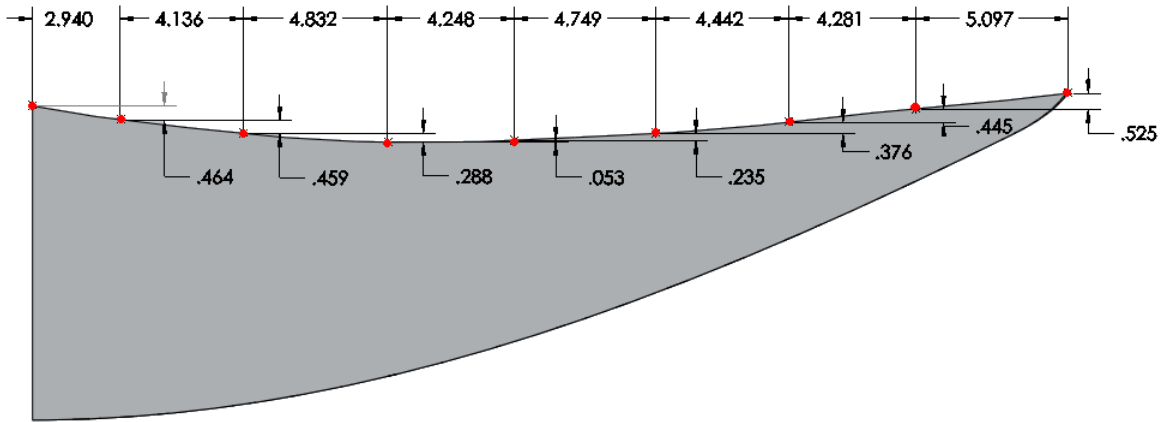
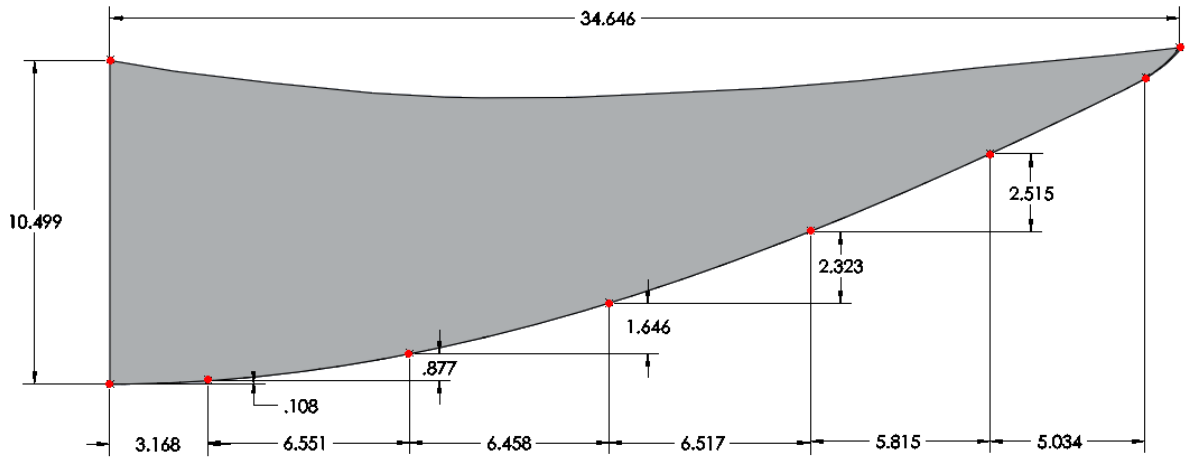
Units in inches unless otherwise specified.



Area: 432.3 in²

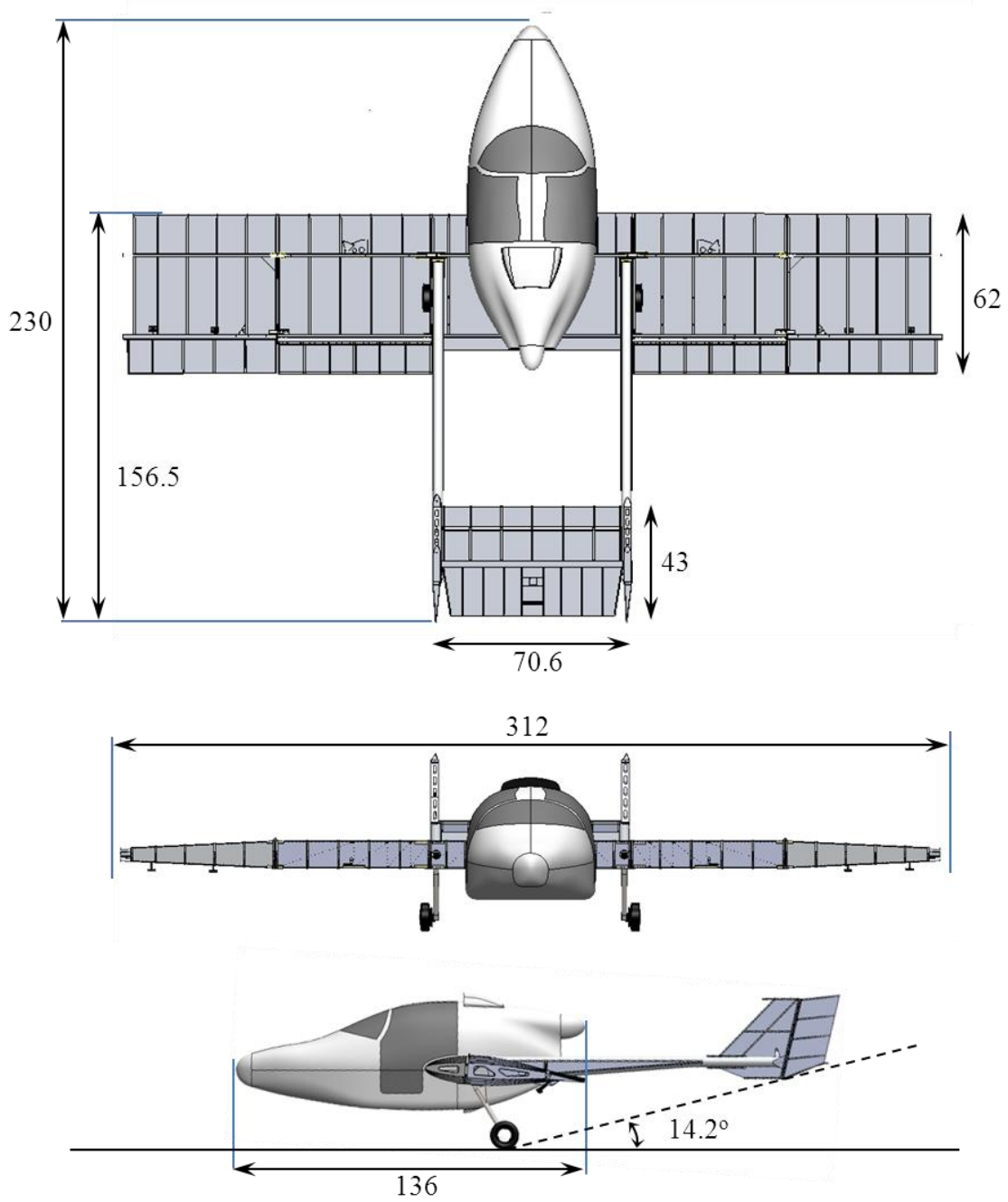
MID-RIB EXTENSIONS

Units in inches unless otherwise specified. Dimensioned points are provided so a spline fit may be re-created to generate the baffle dimensions.



Area: 210.7 in²

Appendix E – New Vampire 3-View



Units in inches unless otherwise specified. Measurements taken from CAD assembly provided by Sadler Aircraft.